HHS Public Access

Author manuscript

Nat Med. Author manuscript; available in PMC 2020 May 26.

Published in final edited form as:

Nat Med. 2019 November ; 25(11): 1772–1782. doi:10.1038/s41591-019-0640-y.

Preventing dysbiosis of the neonatal mouse intestinal microbiome protects against late-onset sepsis

Jeffrey R. Singer[1,9,*], **Emily G. Blosser**[2,7,9], **Carlene L. Zindl**[1], **Daniel J. Silberger**[1], **Sean Conlan**[3], **Vincent A. Laufer**[1], **Daniel DiToro**[1], **Clay Deming**[3], **Ranjit Kumar**[4], **Casey D. Morrow**[5], **Julia A. Segre**[3], **Michael J. Gray**[6], **David A. Randolph**[2,8,10], **Casey T. Weaver**[1,10,*]

[1]Department of Pathology, University of Alabama at Birmingham, Birmingham, AL, USA.

[2]Department of Pediatrics, University of Alabama at Birmingham, Birmingham, AL, USA.

[3]National Human Genome Research Institute, National Institutes of Health, Bethesda, MD, USA.

[4]Center for Clinical and Translational Science Informatics Institute, University of Alabama at Birmingham, Birmingham, AL, USA.

[5]Department of Cell Developmental and Integrative Biology, University of Alabama at Birmingham, Birmingham, AL, USA.

[6]Department of Microbiology, University of Alabama at Birmingham, Birmingham, AL, USA.

[7]Present address: Department of Obstetrics and Gynecology, Ochsner Health System, New Orleans, LA, USA.

[8]Present address: Division of Neonatal-Perinatal Medicine, Rocky Mountain Hospital for Children, Denver, CO, USA.

[9]These authors contributed equally: Jeffrey R. Singer, Emily G. Blosser.

[10]These authors jointly supervised this work: David A. Randolph, Casey T. Weaver.

[*]**Correspondence and requests for materials** should be addressed to J.R.S. or C.T.W. jrsinger@uab.edu; cweaver@uab.edu.

Author contributions

G.B. and D.A.R. conceived of the original model. E.G.B. generated *Kp-43816*^{lux}. J.R.S. generated *Kp-39*^{gfp}. J.R.S. and E.G.B. designed and performed all experiments with guidance from C.T.W., D.A.R. and M.J.G. J.A.S., C.D. and S.C. helped to perform and analyze metagenomics sequencing and strain-tracking experiments. Some immunofluorescence experiments were performed by C.L.Z. Some bioluminescence experiments were performed by D.J.S. D.D. helped prepare figures for the initial submission. V.A.L. fit the statistical models for the analysis of bioluminescence data. 16S rRNA microbiome sequencing and initial analysis were performed by C.D.M. and R.K. J.R.S. analyzed all the data, wrote the original manuscript and prepared the final figures. C.T.W., D.A.R. and J.A.S. secured funding for this project. J.R.S. and C.T.W. authored the final manuscript.

Online content

Any methods, additional references, Nature Research reporting summaries, source data, extended data, supplementary information, acknowledgements, peer review information; details of author contributions and competing interests; and statements of data and code availability are available at https://doi.org/10.1038/s41591-019-0640-y.

Competing interests

The authors declare no competing interests.

Additional information

Extended data is available for this paper at https://doi.org/10.1038/s41591-019-0640-y.

Supplementary information is available for this paper at https://doi.org/10.1038/s41591-019-0640-y.

Peer review information Alison Farrell was the primary editor on this article and managed its editorial process and peer review in collaboration with the rest of the editorial team.

Abstract

Late-onset sepsis (LOS) is thought to result from systemic spread of commensal microbes from the intestines of premature infants. Clinical use of probiotics for LOS prophylaxis has varied owing to limited efficacy, reflecting an incomplete understanding of relationships between development of the intestinal microbiome, neonatal dysbiosis and LOS. Using a model of LOS, we found that components of the developing microbiome were both necessary and sufficient to prevent LOS. Maternal antibiotic exposure that eradicated or enriched transmission of *Lactobacillus murinus* exacerbated and prevented disease, respectively. Prophylactic administration of some, but not all *Lactobacillus* spp. was protective, as was administration of *Escherichia coli*. Intestinal oxygen level was a major driver of colonization dynamics, albeit via mechanisms distinct from those in adults. These results establish a link between neonatal dysbiosis and LOS, and provide a basis for rational selection of probiotics that modulate primary succession of the microbiome to prevent disease.

Neonatal infection is a common cause of infant mortality worldwide, particularly in infants born very prematurely[1,2]. Early-onset sepsis (EOS) occurs within 3 d postpartum and is caused primarily by group B *Streptococcus* (GBS) or *E. coli* acquired during the birth process, whereas LOS is typically caused by commensals of the skin or intestines, including *Staphylococcus* spp., *E. coli*, *Klebsiella pneumoniae* and *Candida* spp.[3]. Mothers in preterm labor who are GBS-positive, or are of unknown status, receive antibiotics empirically to reduce EOS risk and sick preterm infants typically receive empiric antibiotics until EOS is ruled out. Paradoxically, while antibiotic use reduces rates of EOS, it may increase the risk of LOS[4,5], presumably by altering the infant's microbiome.

Primary succession is the sequential population of a new habitat by different species to form an ecosystem. Intestinal microbiome surveys suggest an altered course of primary succession in preterm versus full-term infants[6–10]. Preterm infants often experience overgrowth of a single species from one of the facultative anaerobe bacterial families: Enterococcaceae, Staphylococcaceae or Enterobacteriaceae[6], hereafter referred to as neonatal dysbiosis. It is suggested that sepsis originates from translocation of microbes from the gut[11], and speciation of fecal and blood bacteria indicates that neonatal dysbiosis may set the stage for LOS[12], although a causal relationship has not been established.

Longer gestation correlates with earlier postnatal appearance of obligate anaerobes in the intestinal microbiome[10]. Facultative anaerobes are quickly supplanted by obligate anaerobes during normal succession in term infants[7,9]. However, preterm and very-low-birth-weight (VLBW) infants are sparsely populated by obligate anaerobes, even weeks after birth[6]. Neonatal mice have a similar delay in the appearance of obligate anaerobes[13,14]. Because many features of intestinal development that occur in utero in humans take place postnatally in rodents[15], this suggests that the succession pattern of the microbiome reflects intestinal developmental maturity, which in turn reflects gestational age.

Given the associations between dysbiosis and LOS, clinical efforts have been made to remediate the preterm microbiome by administration of probiotics, typically *Lactobacillus* spp. alone or combined with *Bifidobacterium* spp. or other commensals thought to be

beneficial[16]. While probiotic administration can reduce LOS in VLBW infants[16], choice of the types and dosing of probiotics has been largely empiric and efficacy has proven quite variable[17]. A lack of appropriate animal models for studying LOS has limited understanding of the mechanisms that govern the relationships between intestinal microbiome development in premature infants, neonatal dysbiosis and LOS. Existing models of neonatal sepsis bypass intestinal colonization[18,19], limiting their utility for studies of the role of the microbiome in mitigating infectious risk. Here, we report a mouse model to better study how altered succession of the intestinal microbiome in neonates may predispose to dysbiosis that leads to LOS. Using *K. pneumoniae*, a clinically relevant pathobiont, we identify perturbations in the developing microbiome that facilitate or prevent neonatal dysbiosis and bacterial translocation and dissemination. We find that in vitro measures of probiotic activity do not reliably predict in vivo efficacy, and we identify mechanisms by which select pioneer bacteria may act as probiotics to confer colonization resistance and prevent sepsis. Our findings offer the possibility for rational design and testing of effective probiotic therapies that prevent LOS in susceptible infants.

Results

Neonatal dysbiosis leads to LOS in the absence of adequate host clearance following translocation.

Full-term mice are born less developmentally mature than term humans and their intestines resemble those of premature infants[15]. To model LOS, 5-d-old pups were infected intragastrically (i.g.) with virulent *K. pneumoniae* (ATCC, 43816; *Kp-43816*). This strain was engineered to express bioluminescent[20] (*Kp-43816*^{lux}) or fluorescent[21] (green fluorescent protein, GFP; *Kp-43816*^{gfp}) reporters to enable tissue and histological bacterial imaging, respectively. The administered dose was titrated to cause ~50% mortality in pups reared under specific-pathogen-free (SPF) conditions (Fig. 1a, and data not shown). Using live-animal imaging, real-time colonization and dissemination of *Kp-43816*^{lux} were tracked (Fig. 1b,c). A strong correlation between ex vivo tissue luminescence and isolated *K. pneumoniae* colony-forming units (c.f.u.) validated this approach (Extended Data Fig. 1a,b). The primary sites of infection were localized to the cecum and colon and, to a lesser extent, to the distal small intestine. Monitoring of luminescent bacteria ensured that dosing was limited to the stomach (Extended Data Fig. 1).

Hypothesizing that neonatal dysbiosis precedes sepsis, we predicted finding translocation where pathobiont colonization was most dense. Indeed, 24 h after co-colonization with *Kp-43816*^{lux} and *Kp-43816*^{gfp}, translocation correlated with bioluminescence imaging (Fig. 1d) and *Kp-43816*^{gfp} was found in the livers of septic pups but not in those of pups without sepsis (Fig. 1e). Thus, *K. pneumoniae* dysbiosis led to LOS following intestinal translocation. However, not all pups with dysbiosis developed sepsis, just as not all premature human infants with dysbiosis develop LOS[6].

To better elucidate relationships between neonatal dysbiosis, translocation, host clearance and sepsis, pups were infected with an avirulent strain of luminescent *K. pneumoniae* (*Kp-39*^{lux}; Fig. 1f). *Kp-39*^{lux} showed a similar pattern of colonization to *Kp-43816*^{lux} (Fig. 1g), but with higher luminescence per c.f.u. (Extended Data Fig. 1c). We reasoned that

Kp-39 did not cause LOS owing to either its inability to translocate or its failure to persist extraintestinally. To assess translocation, c.f.u. from the liver and mesentery of nonseptic pups infected with *Kp-43816*^{lux} or *Kp-39*^{lux} were compared. Both before and after development of LOS (days 1 and 3, respectively), more *Kp-43816* than *Kp-39* was recovered from the mesentery, which is seeded via lymphatic spread. However, similar c.f.u. were found for the two strains in the liver, which is seeded via blood (Fig. 1h). Because *Kp-39* was detected in the liver and mesentery on day 1 following infection, we concluded that it could translocate yet not cause sepsis. Accordingly, when introduced intraperitoneally (i.p.) to bypass translocation altogether, *Kp-39*^{lux} also failed to cause sepsis and was cleared within 7 d, whereas all pups infected i.p. with *Kp-43816*^{lux} succumbed within 24 h (Fig. 1i), suggesting that differences in host clearance contributed to the differential virulence of these related strains.

A major virulence factor of *K. pneumoniae* is its polysaccharide capsule, which resists phagocytosis[22]. On the basis of whole-genome sequencing of *Kp-39*, we determined that, whereas *Kp-39* has the less well-studied K10 capsular type, *Kp-43816* is a hypercapsule-producing K2 strain (Fig. 1j), which is known to be resistant to phagocytosis[22]. Accordingly, *Kp-39*^{gfp} was phagocytosed twice as efficiently as *Kp-43816*^{gfp} in vitro (Fig. 1k). We concluded that neonatal dysbiosis leads to LOS after translocated bacteria disseminate in the absence of adequate host clearance. Notably, therefore, while *Kp-43816* infection models LOS, *Kp-39* enables tracking of dysbiosis without the confounding effects of sepsis and mortality.

The microbiome alters susceptibility to neonatal dysbiosis and LOS.

The intestinal microbiome plays a critical role in restraining pathogen colonization and spread[23]. Using our models of LOS and neonatal dysbiosis, we determined whether manipulating the microbiome before infection altered disease susceptibility. Pups without a microbiome, reared in germ-free (GF) conditions, were uniformly susceptible to *Kp-43816*^{lux}-mediated LOS and showed greater colonization than SPF controls (Fig. 2a), indicating that the neonatal microbiome already plays a role in restraining pathobiont growth and dissemination at postnatal day (P) 5. To extend these observations, dams were administered antibiotics to alter the microbiome inherited by their pups. Vancomycin and gentamicin were used to target Gram-positive and Gram-negative bacteria, respectively. Both antibiotics are poorly absorbed and unlikely to be transmitted to pups[24,25]. Dams received antibiotics beginning 1–2 d before delivery and through P4, and pups were infected 1 d later (P5).

Compared to SPF pups, pups of gentamicin-treated dams (henceforth referred to as ‘gent pups’) were markedly more susceptible to development of sepsis, whereas pups of vancomycin-treated dams (henceforth referred to as ‘vanc pups’) were less susceptible (Fig. 2b). To determine whether extraintestinal clearance mechanisms were contributory, antibiotic-reared and SPF pups were infected i.p. with low-dose *Kp-43816*^{lux} (Fig. 2c). All pups succumbed to infection within 24 h, and differences in colonization were observed during only the first 2 h. In contrast to more aggressive antibiotic regimens[18], neither vancomycin nor gentamicin affected extraintestinal clearance of *Kp-43816*^{lux}. We therefore

hypothesized that the effects of maternal antibiotic exposure on neonatal LOS resulted from altered colonization resistance. Consistent with this, *Kp-39*^{lux} infection resulted in higher colonization in gent pups and lower colonization in vanc pups compared to SPF controls (Fig. 2d). These effects were not due to direct antimicrobial activity against *K. pneumoniae*, as gentamicin, which increased mortality, targeted both strains, whereas vancomycin, which protected pups, had no activity against the two strains (Extended Data Fig. 2a). We concluded that maternal antibiotic exposure changed the inherited microbiome, resulting in altered colonization resistance and susceptibility to LOS.

Maternal antibiotics alter communities of perinatally transmitted lactobacilli that confer protection.

The above indicated that perinatal maternal antibiotics altered succession of the neonatal microbiome. We surveyed 16S rRNA sequences from the intestines of P5 pups born to dams administered gentamicin, vancomycin or neither (Fig. 3a). Initial analysis indicated that each microbiome was dominated by relatively few organisms. Despite similar broad trends, principal-component analysis of Bray–Curtis dissimilarities (beta diversity) revealed differences between litters, but also clustering on the basis of antibiotic exposure (Extended Data Fig. 2b). Unbiased analysis of differentially abundant taxa suggested that antibiotic rearing impacted primarily the relative abundance of the *Lactobacillus* and *Rodentibacter* genera (Fig. 3b); the microbiomes of gent pups had greater relative abundance of *Rodentibacter* and lacked *Lactobacillus*, whereas the microbiomes of vanc pups had fewer *Rodentibacter* and greater *Lactobacillus*. Interestingly, SPF pups fell along the spectrum defined by gent and vanc pups (Fig. 3a,b); SPF microbiomes segregated closely with those of either gent or vanc pups. Collectively, this suggested a correlation between presence or absence of lactobacilli and resistance and susceptibility, respectively, to neonatal dysbiosis and LOS.

A limitation of 16S rRNA sequencing data is the inability to determine whether changes in relative abundance of bacterial constituents reflect absolute changes. We therefore complemented sequence analyses with culture-based methods to validate and extend interpretations of sequencing data (Fig. 3c). Results indicated that the sequence data correlated well with c.f.u. enumerated by selective culture analysis. Thus, whereas perinatal administration of gentamicin to dams ablated the population of their pups' lactobacilli, administration of vancomycin enhanced the population of lactobacilli, with *Rodentibacter* remaining unchanged between groups. This suggested a link between the abundance of lactic acid bacteria (LAB) and protection against LOS caused by *K. pneumoniae*.

To determine whether endogenous lactobacilli played a causal role in colonization resistance, we tested whether lactobacilli present in vanc pups could confer protection in gent pups. The contents of colons from vanc pups were cultured under conditions that enriched for endogenous LAB strains, which were administered to gent pups before *K. pneumoniae* challenge (Fig. 3d). Gent pups that received this LAB 'cocktail' showed reduced *Kp-39*^{lux} bioluminescence, indicating that endogenous LAB strains could act as probiotics to provide protection against neonatal dysbiosis.

Because standard 16S rRNA analysis poorly resolves species-level identification of the *Lactobacillus* genus[26], we sought alternative approaches to identify the LAB strain(s) responsible for protection in vanc pups. First, we performed oligotyping analysis on all 16S rRNA gene reads assigned to the Lactobacillales order (Fig. 3e and Extended Data Fig. 3)[27]. This resolved the diversity of 16S sequences to eight oligotypes (Fig. 3e), which could not be fully speciated by 16S analysis (data not shown). In complementary experiments, we isolated 26 colonies with varied morphologies from P5 fecal samples of SPF or antibiotic-treated pups and sequenced the entire 16S rRNA region of each (Fig. 3e). The sequences of individual isolates matched those of three distinct *Lactobacillus* spp.: *Lactobacillus murinus*, *Lactobacillus johnsonii* and *Lactobacillus reuteri*, as well as that of *Streptococcus azizii*, with over 99% similarity to the top BLAST hit (Extended Data Fig. 3c). The 16S sequences derived from the cultured isolates and their unique single-nucleotide variant patterns were used as a custom database for oligotyping analysis. Specifically, of the eight oligotypes resolved from the original 16S rRNA sequence data, five were aligned to isolates with 100% sequence identity and three differed by only a single nucleotide. Thus, we were able to assign these sequences to the species level with high confidence.

On the basis of our speciation results, we determined that the relative and absolute changes in *Lactobacillus* spp. resulting from antibiotic treatment were largely due to changes in abundance of *L. murinus*: the microbiomes of vanc pups were dominated by *L. murinus*, whereas those of gent pups were largely devoid of *L. murinus* (Fig. 3e). Because both gentamicin and vancomycin may inhibit the growth of certain lactobacilli[28], we determined whether differential susceptibilities to these antibiotics might explain reduced versus increased *L. murinus* colonization in gent and vanc pups, respectively[28,29]. Using intestinal isolates of *L. murinus* (strain V10) and *L. johnsonii* (strain G2A), we confirmed that both were sensitive to gentamicin in the presence of bile (Extended Data Fig. 4a,d). At higher doses of gentamicin, increased susceptibility was also observed under aerobic culture conditions (Extended Data Fig. 4b,e). Bile alone had no effect on the growth of either isolate in anaerobic or aerobic environments (Extended Data Fig. 4c,f). This suggested that gentamicin killed protective species of lactobacilli in dams, preventing their passage to pups. In contrast, vancomycin was inactive against *L. murinus* V10 even at high doses (Extended Data Fig. 4b) but showed considerable activity against *L. johnsonii* G2A (Extended Data Fig. 4e). This likely explains why vanc pups are preferentially colonized by *L. murinus* without competition from other vancomycin-susceptible lactobacilli.

Vertical transmission of LAB from mother to infant helps establish the neonatal microbiome[30,31]. To better define the origins of *L. murinus* transmitted from dams to pups, a combined genomic, or metagenomics, approach was used (Extended Data Fig. 5a). Forty-eight isolates collected from control and vancomycin-treated dams and their pups were shotgun sequenced and classified. Overall, 90% of recovered isolates were identified as lactobacilli, 58% of which were *L. murinus* (Extended Data Fig. 5b). *L. murinus* isolates were cultured from only one of four pups examined from control SPF litters. Core single-nucleotide polymorphism (SNP) analysis tightly clustered all three of these isolates with two vaginal isolates from the corresponding dam (Extended Data Fig. 5d). Vancomycin treatment of dams resulted in three pups that were culture positive for *L. murinus*; core SNP

analysis clustered isolates from these pups with maternal isolates in two of the three instances.

These findings confirmed three instances of vertical transmission from dam to pup (Extended Data Fig. 5c), but could not explain a fourth *L. murinus*-positive pup (Extended Data Fig. 5d, starred clade). Because this likely reflected incomplete sampling of the diversity of isolates from the dam, we used shotgun metagenomics to further examine the ensemble of *L. murinus* isolates from the dam and pups. As expected, the contents of the pup colons were dominated by *Rodentibacter* spp. (Fig. 3f). Overall, SPF pups showed low levels of *L. murinus* reads, correlating with their low culture positivity. In contrast, three of four pups from vancomycin-treated dams showed high relative abundances of *L. murinus*, further validating conclusions from oligotyping. When the distribution of core SNPs in the vancomycin-treated dam and pups was examined, it was found that the dam harbored more than one *L. murinus* strain but transmitted a single dominant strain that differed between pups (Extended Data Fig. 5e), again establishing vertical transmission and indicating a stochastic component to engraftment by pioneer species. Because no major differences between vaginal and fecal metagenomes were observed, conclusions about the anatomic origin of the transmitted *L. murinus* strains could not be made.

Select lactobacilli are effective probiotics for prevention of LOS.

In view of the predominance of *L. murinus* in LOS-resistant vanc pups, we tested whether this bacterium might be protective when prophylactically administered to susceptible pups. Gent pups that received *L. murinus* V10 isolated from vancomycin-treated pups showed dramatically reduced overgrowth of *Kp-39*^{lux} compared to controls (Fig. 3g), establishing a potent probiotic effect. Interestingly, this was not generalizable to the commonly utilized probiotics *Lactobacillus rhamnosus* GG (LGG) and *Lactobacillus plantarum* (ATCC, 202195) or to a reference strain of *L. murinus* (ATCC, 35020; Fig. 3g and Extended Data Fig. 6). Notably, pups that received the *L. johnsonii* G2A isolate were also protected but not to the same degree found with *L. murinus* V10 (Fig. 3g). Thus, the probiotic activity of different *Lactobacillus* spp. varied greatly and could not be predicted by absolute quantification of LAB in the intestine after prophylactic treatment or by direct inhibition of *K. pneumoniae* growth in vitro (Extended Data Fig. 7).

A mature microbiome dominated by anaerobes provides resistance to neonatal dysbiosis.

In accordance with results observed in small cohorts of preterm infants[32], we found that pups with less diverse microbiomes were more susceptible to neonatal dysbiosis and LOS (Extended Data Fig. 2b). Moreover, risk factors for LOS in preterm infants that correlate with lower microbiome community diversity[6,10], such as antibiotic use4 and younger gestational age[3], would seem to be similar in our model. We therefore hypothesized that older pups with more diverse microbiome communities would resist neonatal dysbiosis and be protected from LOS. Indeed, we observed that mice rarely developed LOS at P14 or later (Fig. 4a). To assess whether the microbiome was required for the observed age-related protection, recently weaned mice born to dams that were SPF or GF or were colonized with a minimally diverse altered Schaedler flora (ASF) were challenged with *Kp-43816*^{lux}. Although the microbiomes of ASF mice conferred some early resistance to *K. pneumoniae*

overgrowth, ultimately both ASF and GF mice succumbed to infection (Fig. 4b). As before, SPF mice were completely protected.

Having established that SPF pups were protected from LOS beginning at around P14 and that protection was dependent on a more mature microbiome, we surveyed the intestinal microbiome from birth to weaning to define changes in composition. Relative bacterial abundance was heterogeneous in the first days of life when absolute abundance was low (Fig. 4c and Extended Data Fig. 8), but became more homogeneous with age (Fig. 4c and Extended Data Fig. 8). This agrees with previous reports[14,18]. In stratifying the community by oxygen usage (Supplementary Table 1), we observed a shift from communities dominated by facultative anaerobes to those dominated by obligate anaerobes, occurring around week 2 of life and coinciding with protection from LOS. This correlation has also been observed in case–control studies in newborns[33,34]. We therefore reasoned that this shift in the microbiome reflected a transition stage in primary succession, after which the community was less vulnerable to neonatal dysbiosis.

Luminal oxygen drives colonization dynamics and dysbiosis in the neonatal intestine.

In adults, intestinal luminal oxygen is known to drive dysbiosis in the context of antibiotic use, infection and inflammation[35]. We therefore determined whether intestinal oxygen levels decreased with age as mice became less susceptible to *K. pneumoniae* dysbiosis, using the redox chemistry of pimonidazole (PMDZ) to measure epithelial hypoxia[36] (Extended Data Fig. 9a). PMDZ staining of the intestines of control mice showed greater epithelial hypoxia in P21 pups than in P5 or P12 pups (Extended Data Fig. 9b), indicating decreasing luminal oxygen over the developmental window spanning the transition to dominance of obligate anaerobes in the intestinal microbiome and the transition from dysbiosis susceptibility to resistance in mice. This suggested a plausible mechanism for neonatal susceptibility to dysbiosis, as higher oxygen levels favored enhanced growth of *K. pneumoniae* (Extended Data Fig. 9c) and other organisms known to cause neonatal dysbiosis[37].

Epithelial oxygen metabolism triggered by peroxisome proliferator-activated receptor gamma (PPARγ) signaling from Clostridiaderived butyrate is a major pathway that limits oxygen diffusion into the intestinal lumen[38]. If obligate anaerobes imparted protection from LOS to pups as they aged, we speculated that transplanting microbiomes from older pups, who were themselves protected, might reduce the risk of LOS in susceptible pups. In support of this, we found that fecal microbial transplantation (FMT) from P19 donors into gent pups significantly reduced the development of LOS (Fig. 5a) and dysbiosis (Fig. 5b) compared to controls. However, direct butyrate supplementation from treatment with tributyrin was not protective and did not induce gene expression changes indicative of PPARγ activation (Extended Data Fig. 10a,b). Moreover, direct stimulation of PPARγ by rosiglitazone did not impact *Kp-39*^{lux} colonization (Extended Data Fig. 10c,d). These results suggest that pathways restricting luminal oxygen in adult mice are not yet operational in neonates and imply other mechanisms underlying colonization resistance following an FMT.

To determine whether obligate anaerobes could engraft into neonatal recipients, littermate P5 gent pups were administered an FMT (from a P19 donor) or sham treatment for two consecutive days. Adult GF mice received the same FMT. Sequence analysis of donor and

recipient microbiomes 1 d later showed that obligate anaerobes from FMT did not engraft into the neonates, in contrast to observations in GF adults. Rather, the microbiomes of gent pups remained dominated by facultative anaerobes (Supplementary Table 2). Additionally, FMT did not seem to diminish epithelial oxygen (Extended Data Fig. 10e), further suggesting that the neonatal intestine remained aerobic—unable to support obligate anaerobe growth—even after transplantation.

Analysis of FMT recipients showed low relative abundance of Lactobacillales (Fig. 5c). Instead, the microbiomes of FMT recipients were dominated by Enterobacteriales (Fig. 5c), nearly all of which belonged to the genus *Escherichia* (Supplementary Table 2). Thus, in contrast to the protection mediated by bacteria from vanc pups, the protection conferred by P19 FMT seemed to be due to Enterobacteriales, not Lactobacillales. *E. coli*, like *K. pneumoniae*, can act as either a commensal or a pathobiont depending on the strain examined and microbiome context[39,40]. To assess whether *E. coli* engrafted from FMTs could confer protection, a single probiotic strain of *E. coli*, Nissle 1917 (ref. [41]), was evaluated for efficacy in protecting against neonatal dysbiosis (Fig. 5d). Similarly to *L. murinus* (Fig. 3g), *E. coli* Nissle conferred protection in gent pups, confirming that, like some *Lactobacillus* spp., a single probiotic strain of *E. coli* could prevent LOS. These results indicate that diverse bacterial strains may confer colonization resistance against pathobionts that can cause sepsis. They also suggest that strong ecological constraints restrict the engraftment of obligate anaerobes in early life.

Discussion

LOS has been associated with alterations in the developing neonatal microbiome. Here, using a model of LOS, we identify a causal relationship between neonatal dysbiosis and sepsis and define specific antibiotic-induced alterations of the microbiome that predispose to dysbiosis caused by the clinically relevant pathobiont *K. pneumoniae*. Our findings establish that normal constituents of the microbiome are both necessary and sufficient to buffer pathobiont expansion in the neonatal gut to prevent LOS. They further provide a basis for understanding why some probiotics are protective, whereas others are not. This may have important implications for clinical practice, where both maternal[42] and neonatal[43] antibiotic use can alter the neonatal microbiome, and where VLBW infants are given probiotics without clear evidence as to preferred probiotic species.

The prolonged use of broad-spectrum antibiotics in preterm infants has been associated with increased risk of LOS, necrotizing enterocolitis (NEC) and death[4,5]. The unanticipated finding that vancomycin and gentamicin had opposing effects on LOS underscores the importance of better informed antibiotic selection in clinical practice. Notably, empiric antibiotic susceptibility testing is dependent on laboratory conditions[28] and is therefore unreliable when factors present in vivo are not considered (for example, bile). Thus, guidance for clinical antibiotic use could be improved by considering a combined approach that encompasses potential antibiotic activity against the intestinal microbiota and in vivo testing, as well as genetic evaluations[6], and not just in vitro assays.

Despite over a decade of clinical trials[44,45], the lack of a standardized approach to the organism(s), dosage or regimen used has limited probiotic use in neonatal sepsis[17,46]. We found that in vitro growth inhibition of pathobionts did not predict in vivo efficacy. Moreover, while LGG is effective at preventing antibiotic-induced diarrhea in both mice and humans[47], it was ineffective in preventing LOS. In a recent clinical trial, neonatal sepsis was reduced by treatment with a combination of *L. plantarum* and the prebiotic fructooligosaccharide, which is thought to promote engraftment in the neonatal intestine[48]. While we found that *L. murinus* successfully reduced neonatal sepsis in our model, the *L. plantarum* strain and prebiotic used in this clinical trial did not. These results suggest that the therapeutic efficacy of probiotics is highly dependent on ecological context. Given the similarities between the intestines of newborn mice and preterm infants[15], our model offers the possibility of gaining important insights into appropriate selection of probiotics and prebiotics with clinical efficacy against LOS.

The most important ecological parameter highlighted by this study was intestinal oxygen. Elevated luminal oxygen levels have recently been implicated as a major driver of dysbiosis in several inflammatory intestinal pathologies[38]. In adult mice, a positive-feedback loop exists between commensal obligate anaerobes and epithelial cells to maintain low luminal oxygen levels[38]. Butyrate and other products of microbial fermentation signal epithelial cells to promote β-oxidation, increase oxygen consumption and activate transcriptional programs that further reduce luminal oxygen levels[49]. Disruption of this loop by antibiotics or inflammation increases luminal oxygen and results in dysbiosis or increased pathogen virulence, which can be prevented in adult mice by the administration of PPARγ agonists, tributyrin or probiotic strains of *Clostridium*[14,35,50]. Similar approaches to prevent *K. pneumoniae* colonization in our model were ineffective, suggesting that this pathway is not operational in the immature mouse intestine. In view of the paucity of butyrate-fermenting anaerobes and colonic or fecal butyrate in the neonatal mouse[51] and newborn preterm infant[6], respectively, the immature gut and developing intestinal microbiome would seem to be unable to support obligate anaerobes and thus probiotics based on these bacteria. Further caution is warranted because various *Clostridium* species have been associated with NEC[52]. Moreover, even low doses of butyrate or tributyrin were toxic to neonatal mice (data not shown). On the other hand, direct PPARγ agonism has been shown to be effective in a mouse model of NEC[53]. Additional studies will be needed to understand the differences between epithelial cell metabolism in immature versus mature intestines as a basis for targeting host mechanisms that may promote engraftment of obligate anaerobes to resist LOS.

In this regard, we found that mature microbiome communities were reconstituted following FMT into GF adults, but not neonates; obligate anaerobes in FMTs failed to engraft into neonatal intestines. Instead, the microbiomes of neonates that received FMTs were rapidly dominated by facultative anaerobes, particularly *Escherichia* spp.—minor constituents of the donor microbiome. The discrepant engraftment of obligate anaerobes in gent pups and adult GF recipients suggests that higher oxygen levels in the neonatal intestine are a barrier. This is in accordance with findings presented herein and by others[54] that the intestines of adult GF mice are more hypoxic than those of neonates, despite previous work supporting a role for the microbiome itself in creating the low oxygen tensions in mature mice[49]. Additionally,

dietary sugars in maternal milk may impact the developing microbome[9] and could contribute to a lack of support for growth of obligate anaerobes. This will need to be explored further. In any case, our findings indicate that both the composition of the microbiome and host factors that change with age independently of a commensal flora play important roles in establishing luminal oxygen levels. Thus, although adult GF mice are often used to model primary succession of the intestinal microbiome and its interactions with the host[14], intrinsic support of obligate anaerobes in the intestines of adult mice seems to be an important limitation to the use of these mice in modeling neonatal sepsis.

Remarkably, we found that a single species of *Lactobacillus*, *L. murinus*, consistently dominated the microbiome of neonatal mice born to dams treated with vancomycin and was an effective probiotic monotherapy in preventing LOS. The vertical transmission of *L. murinus* from vancomycin-treated dams to their pups provides evidence that the inherent antibiotic resistance of different lactobacilli underlies the dominance of *L. murinus* in protected neonates. While more work is needed to resolve the timing and anatomic source of this transmission, including the possibility of prepartum microbial transmission, which has been suggested in some human studies but remains controversial[55], our results establish a causal relationship between the colonization of neonates by endogenous *Lactobacillus* spp. and pathobiont colonization resistance. They further establish that a single strain of *Lactobacillus* can be an effective probiotic in this model.

Importantly, not all *Lactobacillus* species were protective, including commercial probiotic strains. While *L. murinus* V10 prevented neonatal dysbiosis, *L. murinus* ASF 361 (as a component of ASF) and *L. murinus* ATCC 35020 failed to protect against dysbiois in adults and in neonates, respectively. *Lactobacillus* is a highly diverse genus with marked differences in the capacity of individual species for aerobic metabolism[56]. In view of the correlation between protection by certain *Lactobacillus* spp. and their induction of increased epithelial hypoxia, we hypothesize that there are links between the capacity of *L. murinus* for aerobic metabolism and its capacity for altering primary succession in immature intestines. Nevertheless, even lactobacilli that have a functional respiratory chain often require exogenous cofactors like heme or menaquinones for respiration, which can be limiting. Consequently, some fermentation may occur even in aerobic environments[56]. Fermentation products of lactobacilli have been explored as probiotic effectors[57–59], and this attribute of lactobacilli may further contribute to their function as a beneficial pioneer species in the oxygen-rich neonatal intestine.

Additional studies will be required to understand the basis for the probiotic efficacy of some, but not other, strains of lactobacilli. However, the identification of different strains of *Lactobacillus* spp. with distinct probiotic efficacies should enable definitive testing of the contribution of bacterially induced alterations in intestinal oxygen tensions to probiotic efficacy in our model and ultimately in the clinic. Because a large consortium of whole-genome sequence data exists for endogenous and commercial lactobacilli, a comparative genomics approach to identify potential genes and pathways involved in probiotic activity is now feasible. This should enable identification of gene targets for generation of isogenic mutants to be tested for probiotic activity and should aid in delineation of mechanisms by which lactobacilli exert their probiotic activity in LOS.

Finally, it should be emphasized that lactobacilli were not unique in preventing dysbiosis in our model. A probiotic strain of *E. coli* achieved protection that matched or exceeded that provided by *L. murinus* as a monotherapy. Although it was recently reported that commensal and probiotic Enterobacteriaceae ameliorated *Salmonella* infection by competing for oxygen[60], we found that FMT led to the engraftment of native *E. coli* strains that were protective without a reduction in intestinal oxygen levels. Thus, mechanisms in addition to reduction of oxygen tension can confer resistance to overgrowth of pathobionts that thrive in the neonatal gut. This raises the possibility of independent and potentially synergistic mechanisms by which different bacterial species may cooperate in the prevention of LOS, whether owing to oxygen reduction or other mechanisms. Our development of a mouse model with which to screen candidate bacteria and elucidate mechanisms by which they act should lead to more rational design of probiotic therapeutics to protect at-risk premature infants. It should further provide an opportunity to define mechanisms by which pioneer species of the developing microbiome of neonates prevent, or fail to prevent, neonatal dysbiosis that predisposes to LOS.

Methods

Bacteria.

Generation of *Kp-43816*^{lux}.—Bioluminescent *K. pneumoniae* ATCC 43816 were generated by Tn7-transposon-mediated chromosomal integration of a luciferase cassette from plasmid pBEN276 as described[20]. Briefly, *K. pneumoniae* ATCC 43816 were grown to log phase and washed with sterile water four times before electroporation with pBEN276, which was generously provided by P. Germon (Unité Infectiologie Animale et Santé Publique) and M. Lawrence (Mississippi State University)[61]. A Gene Pulser II (Bio-Rad) was used for electroporation with settings of 2.5 kV, 25 μF and 400 Ω. Colonies were selected on LB plates with high-dose ampicillin for 16 h at 30 °C. Resistant colonies were cultured in LB with arabinose for 16 h at 30 °C to initiate transposition. Cultures were streaked onto LB plates, which were incubated for 16 h at 42 °C to cure the plasmid. Plates were then imaged and screened for bioluminescence. Bioluminescent colonies were cultured in broth for 2 h at 42 °C once more and screened again for loss of ampicillin resistance to verify successful chromosomal insertion.

Generation of Kp-39^{gfp}.—GFP-expressing *K. pneumoniae Kp-39*^{gfp} were generated by Tn7-transposon-mediated chromosomal integration of a GFP coding sequence subcloned from the plasmid cassette pSMC21 with the addition as previously described[62]. pSMC21 was generously provided by G. O'Toole (Dartmouth University). The *frr* gene promoter was added in front of the *gfp* cassette using restriction cloning after amplifying *frr* from *K. pneumoniae* ATCC 43816 genomic DNA with Phusion high-fidelity polymerase (NEB) and XhoI (NEB) digestion of the pSMC21 plasmid. The *frr*-forward sequence was 5′-GTCTGACTCGAGGAATTCTTCCCGTGATGGATAAATAAG-3′ and the *frr*reverse sequence was 5′-CATCACTCGAGGTTACGAATCCTTGAAAACTTG-3′. PacI restriction sites were added flanking the *frr-gfp* cassette with Phusion high-fidelity polymerase (NEB) and the entire cassette was subcloned into a pCR-Blunt II-Topo backbone (ThermoFisher). The PacI-*gfp*-forward sequence was 5′-CAAGGCGATTAAGTTGGGTAACG-3′ and *the*

PacI-*gfp*-reverse sequence was 5′-GGCTTTACACTTTATGCTTCCGG-3′. The final Tn7-*gfp* vector (pTn7-*gfp*) was then generated by restriction cloning following PacI digestion of both the *frr-gfp* cassette and pGRG36 plasmid. The Gene Pulser II (Bio-Rad) was used for electroporation with settings of 2.5 kV, 25 μF and 400 Ω. Colonies were selected on LB plates with ampicillin (100 μg ml^{-1}) for 16 h at 32 °C. Plates were then imaged using Illumina IVIS and GFP-positive colonies were re-streaked on LB at 42 °C for single-colony isolation and to ensure complete loss of plasmid. All subcloning steps were verified by restriction digest and Sanger sequencing to ensure no mutations were added during amplification steps.

Probiotic supplementation.—Overnight anaerobic cultures of *Lactobacillus* strains grown in 5 ml of MRS broth were washed and diluted with sterile PBS. A final dose of ~10^6 c.f.u. for each organism was gavaged i.g. on P5 and again on P6. For each treatment, a test dose was serially diluted and plated to confirm between 1×10^5 and 5×10^7 c.f.u. were delivered. *E. coli* Nissle was grown aerobically overnight in 5 ml of LB at 37 °C and 250 r.p.m. and the test dose was determined on LB or MacConkey agar. To prepare FMT, feces from P19 pups were collected and homogenized in sterile PBS or Cary Blair medium (5 g l^{-1} NaCl, 1.5 g l^{-1} sodium thioglycolate, 1.1 g l^{-1} Na_2HPO_4, 0.1 g l^{-1} $CaCl_2$). Homogenates were centrifuged at 500*g* for 20 min and supernatants were collected and stored at −80 °C until use. FMTs were frozen at a final concentration of one pellet per 100 μl of medium and a 50-μl dose of FMT or control medium was used per treatment.

Growth curves.—Single colonies of each lactobacilli or *K. pneumoniae* strain were picked from overnight anaerobic growth on MRS agar or aerobic growth on MacConkey agar. Overnight cultures were prepared in 5 ml of the same medium and the same oxygen tension was used the following day for growth curve analysis. Cultures were diluted in fresh medium to OD_{600} of 0.1 and measured for growth every hour for 24 h in triplicate wells of a 96-well plate. Media included MRS with or without 0.01% bile acids (Sigma) or minimal medium (1× M9 salts (Difco), 200 μM $MgSO_4$, 20 μM $CaCl_2$) with 4 g l^{-1} glucose or 10 g l^{-1} casamino acids (Fisher BioReagents) as the sole carbon source.

Mice.

The C57BL/6J mouse colony was bred and maintained at the University of Alabama at Birmingham (UAB). Colony husbandry and all of the experiments involving mice were approved by UAB's Institutional Animal Care and Use Committee. In experiments not requiring gnotobiotic isolators, timed matings of littermate females were employed when comparing pups born in different litters. For experiments with antibiotic-treated dams, timed pregnant littermates were co-housed for the duration of their pregnancies without males until embryonic day (E) 19 or E20. Fresh hydropacs were weighed and impregnated with antibiotics to a final concentration of 1 g l^{-1} vancomycin or 0.1 g l^{-1} gentamicin and pregnant females were gavaged i.g. with a loading dose of 50 mg and 5 mg, respectively. Antibiotics remained in the drinking water until P4 or P5 depending on the experiment. For experiments comparing probiotic supplementation or fecal transplantation, 2–3 dams who gave birth on the same day were co-housed with their pups through the remainder of the experiment. Pups were randomly assorted into groups before their first treatment.

K. pneumoniae dysbiosis and sepsis infection model.

K. pneumoniae were grown aerobically overnight in LB (10 g l^{-1} protease peptone 3, 5 g l^{-1} yeast extract, 10 g l^{-1} NaCl) at 37 °C and 250 r.p.m. The following day, the culture was diluted 1:50 in fresh LB and left for 2–3 h to reach exponential growth phase. Bacteria were washed twice with sterile PBS and resuspended to deliver 10^7 c.f.u. per 50-µl dose i.g. via a 22-gauge flexible polypropylene gavage needle (Instech). For each experiment, a test dose was serially diluted and plated to confirm between 5×10^6 and 5×10^7 c.f.u. were delivered. Between each animal, the gavage needle was sanitized with 10% bleach and/or 70% ethanol, and then dipped in sterile PBS for lubrication. Animals were imaged within 6 h of infection with the IVIS Lumina imaging system. Pups with luminescence signal in the thoracic cavity were killed and removed from the experiment. Litters were observed and imaged one to two times daily throughout the remainder of each experiment. Septic pups were removed immediately and clean bedding was provided daily to prevent cannibalism.

K. pneumoniae intraperitoneal sepsis model.

K. pneumoniae were prepared as with i.g. infection, but resuspended to deliver either 10^5 or 10^3 c.f.u. per 50-µl dose i.p. using a 28-gauge insulin syringe (BD). For each experiment, a test dose was serially diluted and plated to confirm the c.f.u. delivered. Pups were followed closely over the next 10 d for bioluminescence signal and mortality. In each litter, at least two pups remained uninfected.

Bioluminescence imaging.

Pups were removed from their mother and anesthetized on a heated platform in a fabricated anesthesia chamber using inhaled 3–4% isoflurane gas mixture with an oxygen flow rate of 3 l min^{-1}. Animals were imaged on their abdominal side for an exposure of 1–3 min. If extra-abdominal luminescence was detected, pups were killed and removed from the litter. If body temperature decreased during imaging, pups were rewarmed before returning to their mothers. Images were analyzed using LivingImage software and regions of interest (ROIs) were drawn to cover the entire abdomen. Luminescence was measured as average radiance per second (p s^{-1} cm^{-2} sr^{-1}), where p corresponds to photons, cm^2 is the area of the ROI and sr represents the squared radian of the ROI. For some experiments, after whole-body imaging, pups were killed and organs were removed for immediate ex vivo imaging. Organs were arranged on Petri dishes and imaged with a reduced exposure time (10 s min^{-1}).

K. pneumoniae c.f.u. determination.

Following bioluminescence imaging, intestinal and extra-intestinal organs were transferred to a pre-tarred tube with 1 ml of sterile PBS. Tissue was homogenized using PowerGen500 (Fisher), serially diluted in sterile PBS, and plated on MacConkey agar overnight at 37 °C in ambient air. Dilutions with between 30 and 300 colonies were recorded for colony counts the following morning. During homogenization, the homogenizer was cleaned with 70% ethanol and water between samples, and both blank and uninfected organs were used as negative controls.

Phagocytosis assay.

J774A.1 macrophages (ATCC TIB-67) were grown in complete DMEM supplemented with 10% FBS, 100 IU ml^{-1} penicillin and 100 μg ml^{-1} streptomycin (Invitrogen). Cells were seeded in a 12-well plate with antibiotic-free medium 15 h before beginning the assay at 10^6 cells per well. Exponential-growth-phase *Kp-39*^{gfp} or *Kp-43816*^{gfp} were added to macrophages and centrifuged to bring them into contact with cells. After 1 h at 37 °C, gentamicin (Sigma) was added to a final concentration of 100 μg ml^{-1}. Following another hour of incubation, the medium was removed and macrophages were washed vigorously three times with sterile PBS to detach cells from each well. Samples were stained and analyzed on an Attune NxT flow cytometer. FCS files were further analyzed using FlowJo v.9.8.2.

PMDZ hypoxia assay.

Pups were injected with 60 mg kg^{-1} PMDZ HCl (Hypoxyprobe) in sterile PBS. After 1 h, colons were removed, flushed with ice-cold PBS and fixed overnight in 4% paraformaldehyde. The following day, tissue was transferred to PBS for two 12-h incubations at 4 °C and finally into 30% sucrose solution overnight. The following day, colons were snap-frozen in tissue molds filled with OCT medium (Tissue-Tek) in an isopentane (Sigma) bath and left at −80 °C until further processing. Colons were cryosectioned and blocked for endogenous binding with biotin or avidin (Vector Labs) and nonspecific antibody binding with 10% mouse serum. Sections were then stained overnight at 4 °C with anti-PMDZ (clone 4.3.11.13). We applied streptavidin-conjugated AF555 (Invitrogen) as a secondary stain and counterstained with ProFade Gold with DAPI (Invitrogen) before imaging on a Nikon Eclipse E800 fluorescence microscope. Images were analyzed within 24 h of staining. Overall, 5–6 image fields were randomly selected from mid-colon (×20 magnification). PMDZ fluorescence intensity was measured across surface epithelial cells using Fiji software with ROIs drawn contiguously around surface epithelial cells. To normalize for tissue thickness and staining variation, DAPI intensity was compared for each region.

Colony isolation and identification.

Intestinal tissue from 5-d-old pups was transferred into a pre-tarred tube with 1 ml of sterile PBS. Tissue was homogenized using PowerGen500 (Fisher), serially diluted in sterile PBS and plated on BHI (Difco) and MRS (Difco) agar overnight at 37 °C in a container with BD GasPakEZ (anaerobic) or ambient air (aerobic). Dilutions with between 30 and 300 colonies were recorded for colony counts after 24 h. Agar plates were assessed for colonies with different colony morphologies. Over two dozen colonies from three separate experiments were kept as isolates after additional re-streaking to confirm single-colony identity. The whole 16S rRNA gene was then amplified from each isolate using 500 nM 8F (5′-AGAGTTTGATCCTGGCTCAG-3′) and 1492R (5′-GGTTACCTTGTTACGACTT-3′) with Phusion high-fidelity polymerase (NEB) under the following reaction conditions: initial denaturation at 98 °C for 3 min; 34 cycles of denaturation at 98 °C for 30 s, annealing at 53 °C for 30 s and extension at 72 °C for 30 s; and final extension at 72 °C for 3 min. Amplicons from each reaction were column purified (Qiagen) and subjected to Sanger

sequencing spanning the entire region. The consensus sequence for each isolate was then determined, and the sequence was classified using BLAST against the NCBI 16S rRNA gene database (with a sequence identity of 98–100%).

16S rRNA gene microbiome sequencing analysis.

To avoid potential contamination and error from using a small amount of starting materials, DNA was extracted from up to 250 mg of whole intestinal tissue. The intestinal tract from the duodenum to the rectum was aseptically excised, cleaned of mesentery and placed in a sterile, pre-tared microfuge tube. Tissue was partially homogenized with autoclaved scissors, and DNA from up to 250 mg of sample was immediately extracted using the MoBio/QIAamp PowerFecal kit according to the manufacturer's instructions or kept at −80 °C until further processing. DNA was quantified using a NanoDrop, and samples were diluted to 2.5 ng μl^{-1} in MQ water. The V4 region of the 16S rRNA gene was amplified and sequenced using the MiSeq platform as previously reported[63]. The 250-bp amplicons were sequenced and raw FASTQ files were analyzed using the DADA2 pipeline of Nephele v.2 for each of the three analyses. Relative abundances were then generated for order-level taxonomy. The following experiment-specific analyses were also performed.

Microbiome survey with antibiotic exposure.—Alpha-diversity metrics were calculated from a biom file using QIIME v.1.9.1 (ref. [66]). Data were analyzed using standard pipelines with linear discriminant effect size (LEfSe) galaxy cluster[64]. For oligotyping analysis, FASTQ files were first processed using the QWRAP and QIIME pipeline as previously described[63]. Briefly, chimeras were filtered from sequencing data using USEARCH and de novo clustering was then performed at 97% identity using UCLUST. Representative operational taxonomic units (OTUs) were picked on the basis of abundance and assigned taxonomic classification from the RDP Classifier at a threshold of 0.8 and the Greengenes database. Next, we used q2oligo.py[65] to extract all reads assigned to the Lactobacillales order or the Gammaproteobacteria class after chimera filtering and before clustering. Using standard oligotyping pipelines described by Eren et al.[27], initial entropy was calculated for each group. Gammaproteobacteria had little unexplained entropy, and therefore no further steps were taken to oligotype this taxonomy. Lactobacillales had marked unexplained entropy at numerous positions, and oligotyping was iterated six times until it was determined that five oligotypes best resolved sequence diversity into ecologically meaningful categories. Each oligotype was then aligned to the full 16S gene sequence from each neonatal intestinal isolate. Four of the five Lactobacillales oligotypes and the single Gammaproteobacteria oligotype matched at least one 16S rRNA gene from an intestinal isolate with 100% sequence identity. One of the five Lactobacillales oligotypes that did not match intestinal isolates contained a single-nucleotide difference and had over 99% identity to intestinal isolates (potentially reflecting a sequencing error).

Microbiome survey with age and fecal transplant.—Genus-level taxonomies were classified as aerobe, facultative anaerobe or obligate anaerobe according to previous work[66–68] and summed to generate a total relative abundance for each category in a given sample.

Genome sequencing.

Library preparation for Illumina MiSeq and single-molecule real-time (SMRT) sequencing was performed as described previously[69]. Pairedend MiSeq reads were assembled into contigs by using SPAdes v.3.11.1 (ref. [70]) and further polished by using Pilon v.1.22. PacBio Sequel sequencing reads (Sequel Sequencing kit v.3.0 chemistry, 600-min collection) were assembled by using CANU v1.8 (ref. [71]) or HGAP4 (PacBio SMRT Link v.6.0 software). The resulting PacBio read contigs were polished with Arrow (PacBio SMRT Link v.6.0 software). Genome annotation was performed using the NCBI Prokaryotic Genome Annotation Pipeline (https://www.ncbi.nlm.nih.gov/genome/annotation_prok/). Core SNPs were identified using ParSNP[72]. SNPs in recombinant regions were removed using the PhiPack option in ParSNP, and additional large recombinant regions associated with, for instance, phage were manually removed. Capsular typing analysis for *K. pneumoniae* genomes was performed using Kaptive software with standard settings[73].

Metagenomics.

DNA was extracted from dam culture-enriched metagenomes (see description by Johnson et al.[74]) and pup total colon contents, using the QIAamp PowerFecal DNA kit. Libraries were prepared using the Illumina Nextera kit, quantified by NanoDrop and pooled for sequencing on an Illumina NextSeq using 2 × 151 nucleotide paired-end reads (median insert size range: 170–277 nucleotides); on average, 6.9 million read pairs per sample were obtained. Sequences were trimmed with cutadapt v.2.1 and aligned to the mouse genome to remove host sequences. Microbial reads were classified using Kraken2 v.2.0.7-beta[75]. Isolate diversity was estimated for 187 core SNP positions, identified in the ParSNP analysis, by aligning metagenomic reads to the reference genome with Bowtie[76] and extracting allele frequencies using bam-readcount (https://github.com/genome/bam-readcount).

Quantitative PCR.

Whole-colon tissue from P7 pups was collected, trimmed of mesentery and flushed gently with ice-cold PBS to remove colon contents. Tissue was then placed in 1 ml of QIAzol (Qiagen) and homogenized using PowerGen500 (Fisher). RNA was extracted using the RNeasy Mini kit (Qiagen) according to the manufacturer's instructions, including on-column DNase digestion. RNA (500 ng) from each sample was used as a template for cDNA synthesis with iScript supermix (Promega), and the reaction was then diluted fivefold in DNase-free water. Triplicate 10-μl reactions (1× supermix, 300 nM forward and reverse primers, 5 μl of cDNA) were carried out on CFX96 (Bio-Rad) using SSOAdvanced Universal SYBR Green Supermix (Bio-Rad) under the following reaction conditions: 95 °C for 1 min followed by 39 cycles of 95 °C for 5 s and 60 °C for 30 s. Relative qPCR expression was analyzed using the average threshold cycle from triplicate wells for each gene of interest compared to the threshold cycle for *hprt1* in the same sample, calculated as $2^{\wedge}(Ct_{hprt1}-Ct_{GOI})$.

Immunofluorescence imaging.

Colons were removed and lumens were delicately infused with ice-cold PBS and subsequently with 4% paraformaldehyde so as not to dislodge fecal material in the intestinal

tract. Tissue was then kept in 4% paraformaldehyde at 4 °C overnight. The following day, tissue was transferred to PBS for two 12-h incubations at 4 °C and finally into a 30% sucrose solution overnight. The following day, colons were snap-frozen in tissue molds filled with OCT medium (Tissue-Tek) in an isopentane (Sigma) bath and left at −80 °C until further processing. Colons were cryosectioned and blocked for endogenous biotin or avidin binding activity (Vector Labs) and nonspecific antibody binding with 10% mouse serum. Sections were then stained overnight at 4 °C with biotin-conjugated anti-CD326/EpCAM (eBioscience, clone G8.8). We applied streptavidin-conjugated AF555 (Invitrogen) as a secondary stain and counterstained with ProFade Gold with DAPI (Invitrogen) before imaging with a Nikon A1R confocal microscope. Livers were immediately fixed in 4% paraformaldehyde and subsequently treated as for the colons. Cryosectioned tissue was counterstained with DAPI, and no further staining was performed. Slides were imaged on a Nikon Eclipse E800 fluorescence microscope.

Antibiotic susceptibility assay.

The same general protocol was applied for all antibiotic testing. Discs 7.5 mm in diameter (Whatman filter paper no. 1) were punched with a metal hole punch and autoclaved. Then, 5 μl of sterile-filtered water, vancomycin or gentamicin was added to each disc in a biosafety cabinet and discs were left to stand for 30 min. Using autoclaved forceps, discs were placed in the center of each 10-cm agar plate (1.5% agar) and pressure was applied gently. Each experimental condition was assayed in triplicate. Overnight bacterial culture was inoculated and mixed into autoclaved 0.7% agar cooled to 50 °C with a final OD_{600} of 0.1. Five milliliters of bacteria–agar mixture was added to the top of each plate and allowed to set. Following growth for 12–24 h at 37 °C in room air (aerobic) or in a closed vessel with BD GasPakEZ (anaerobic), plates were imaged and the diameter of inhibition was measured. *K. pneumoniae* were grown aerobically overnight in LB with agitation, and diffusion assays were performed on MacConkey agar. Lactobacilli were grown anaerobically overnight in MRS broth (Difco) without agitation and with or without 0.01% bile (Sigma), and diffusion assays were performed on MRS agar with or without 0.01% bile.

Agar overlay assay.

MRS agar plates were left with their lids removed in a biosafety cabinet for 30 min before beginning the assay to dry out the plates. Overnight anaerobic cultures of *Lactobacillus* strains were diluted to a final OD_{600} of 0.5 in fresh MRS medium. Then, 5 μl of each strain was added to the center of an agar plate and left to dry for 5 min. Plates were grown for 24 h at 37 °C in a closed vessel with BD GasPakEZ (anaerobic). The following day, overnight culture of *K. pneumoniae* was inoculated and mixed into autoclaved 0.7% MRS agar cooled to 50 °C with a final OD_{600} of 0.1. Five milliliters of the bacteria–agar mixture was gently added to the top of each plate where spot lactobacilli colonies had grown from the previous day and was allowed to set. Following growth for 24 h at 37 °C in room air, plates were imaged and the diameter of inhibition was measured. Each experimental condition was assayed in triplicate.

Sample size and statistics.

Statistical analysis was performed using GraphPad Prism software v.7 and the computer programming language R. Asterisks are used to indicate statistical significance as follows: $*P \leq 0.05$; $**P \leq 0.005$; $***P \leq 0.0005$; and $****P \leq 0.0001$.

c.f.u. statistical modeling.—For c.f.u. data, all statistical tests used the nonparametric Mann–Whitney *U*-test or Kruskal–Wallis analysis of variance with Dunn's multiple-comparisons correction for comparing two and three groups, respectively.

Survival data.—Between-group survival comparisons were made with a log-rank test for significance with Bonferroni adjustment.

Bioluminescence statistical modeling.—We tested the relationship between luminescence and microbiome groups for statistical significance first using fixed-effects linear modeling. However, because littermates were included in these experiments, we accounted for non-independence stemming from shared environment and genetics by linear mixed modeling. To do this, general linear mixed models were fitted to the data for each experiment using the lmer function within the lme4 package in R[77]. Specifically, we regressed the log of luminescence on microbiome type, further considered the sex of each pup and the experimental ID as covariates, and included a random intercept for the litter.

Model diagnostics.—Generalized linear mixed models (Gaussian family; identity link) were fitted to the data by the reduced maximum likelihood approach. Model fit was assessed by visual analysis of histograms of residuals and by testing them for normality using Shapiro–Wilk's tests before using each model.

Statistical significance.—Satterthwaite's method for Student's *t*-tests was used to assess the statistical significance of the relationship between microbiome group and log luminescence as used in the lme4 package.

Plots.—Box-and-whisker plots show median and IQR, with lines extending to the first and fourth quartiles.

Reporting Summary.

Further information on research design is available in the Nature Research Reporting Summary linked to this article.

Data availability

The whole-genome sequencing data of *L. murinus* isolates and metagenomics sequencing data for this study are linked to NCBI BioProject number PRJNA542320. The 16S rRNA sequencing data for this study are linked to NCBI BioProject number PRJNA587139. All other data are available upon reasonable request without restrictions.

Extended Data

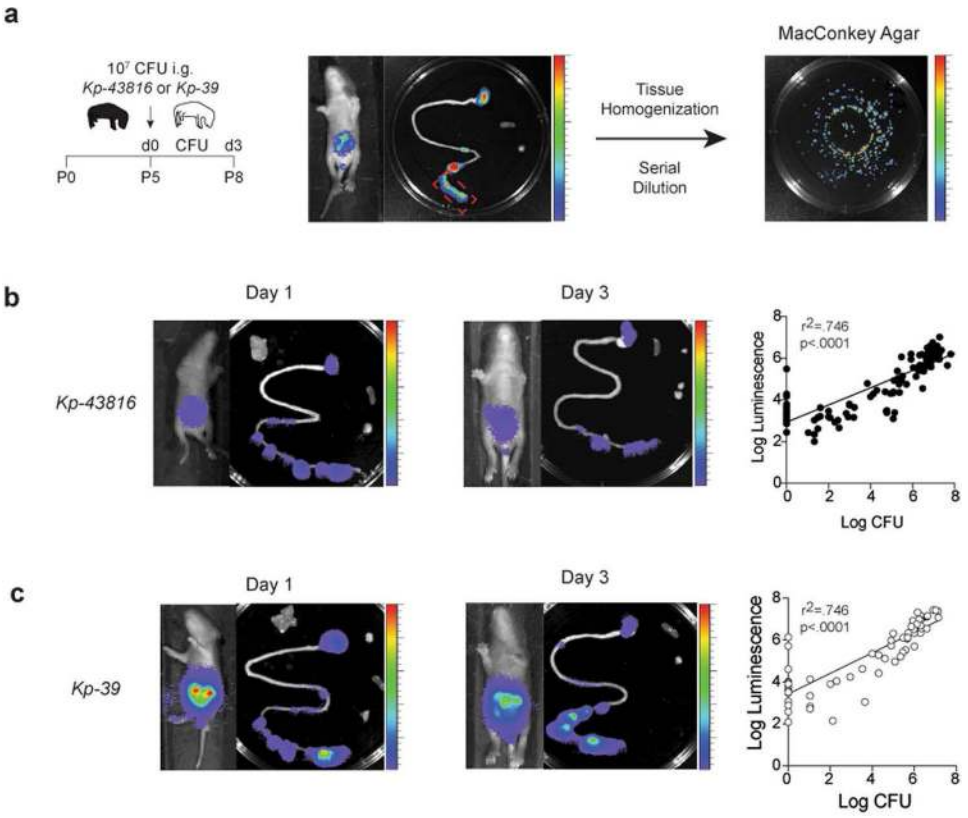

Extended Data Fig. 1 |. *K. pneumoniae* bioluminescence correlates with CFU.

(**a**) Schematic illustration for *K. pneumoniae* infections. Litters of pups (n = 6–12) were infected intragastrically (i.g.) with 107 CFU Kp-43816 or Kp-39 on P5. On day 1 or day 3 following infection, intestinal organs were removed, luminescence signal measured, homogenized, and CFU determined by selective plating on MacConkey Agar. All colonies grown on MacConkey Agar were bioluminescent (right). Representative images of pups infected with Kp-43816 (**b**) and (**c**) and correlation between luminescent signal and CFU for each organ isolated. Each point in (b) and (c) represents an individual organ (small intestines, colon, cecum, mesentery, or liver) from a mouse infected with Kp-43816 (b) collected on day 1 (n = 21) or day 3 (n = 15) post infection, or infected with Kp-39 an day 1 (n = 9) or day 3 (n = 6). Regression analysis performed using ordinary least squares model on log-transformed CFU and bioluminescence data. P values were calculated to test the null hypothesis that the slope of regression line = 0. Number of pups of either sex, n.

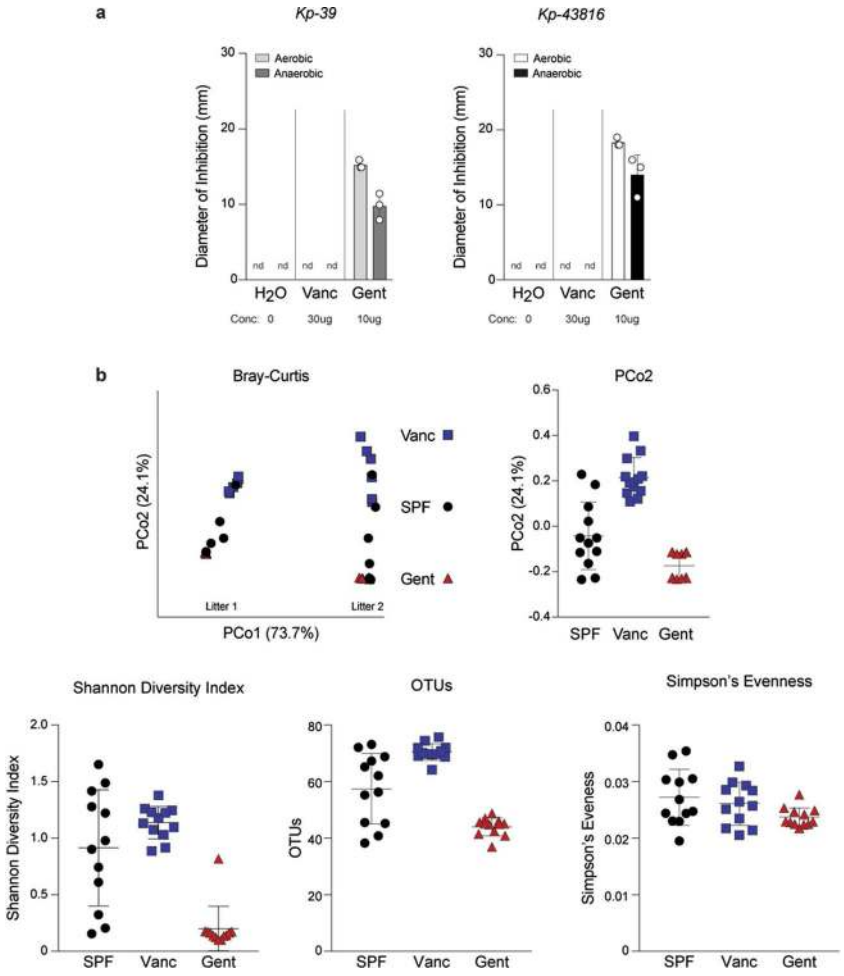

Extended Data Fig. 2 |. *K. pneumoniae* susceptibility to perinatal antibiotics that alter diversity of the neonatal intestinal microbiome.

(a) Growth inhibition disk diffusion assay showing antibiotic susceptibility of Kp-39 (left) and (right) to vancomycin (30ug) or gentamicin (10ug) grown under aerobic or anaerobic conditions. Bars display mean ± SD. No inhibition detected, nd. Data representative of 3 similar experiments; n = 3 plates per condition tested. (b) Beta-diversity (upper panel) and alpha-diversity (lower panel) measurements from microbiome communities of P5 pups reared with or without maternal antibiotics. Lines display mean ± SD. Beta-diversity and alpha-diversity metrics were calculated from the microbiome sequencing data described in Fig. 3a.

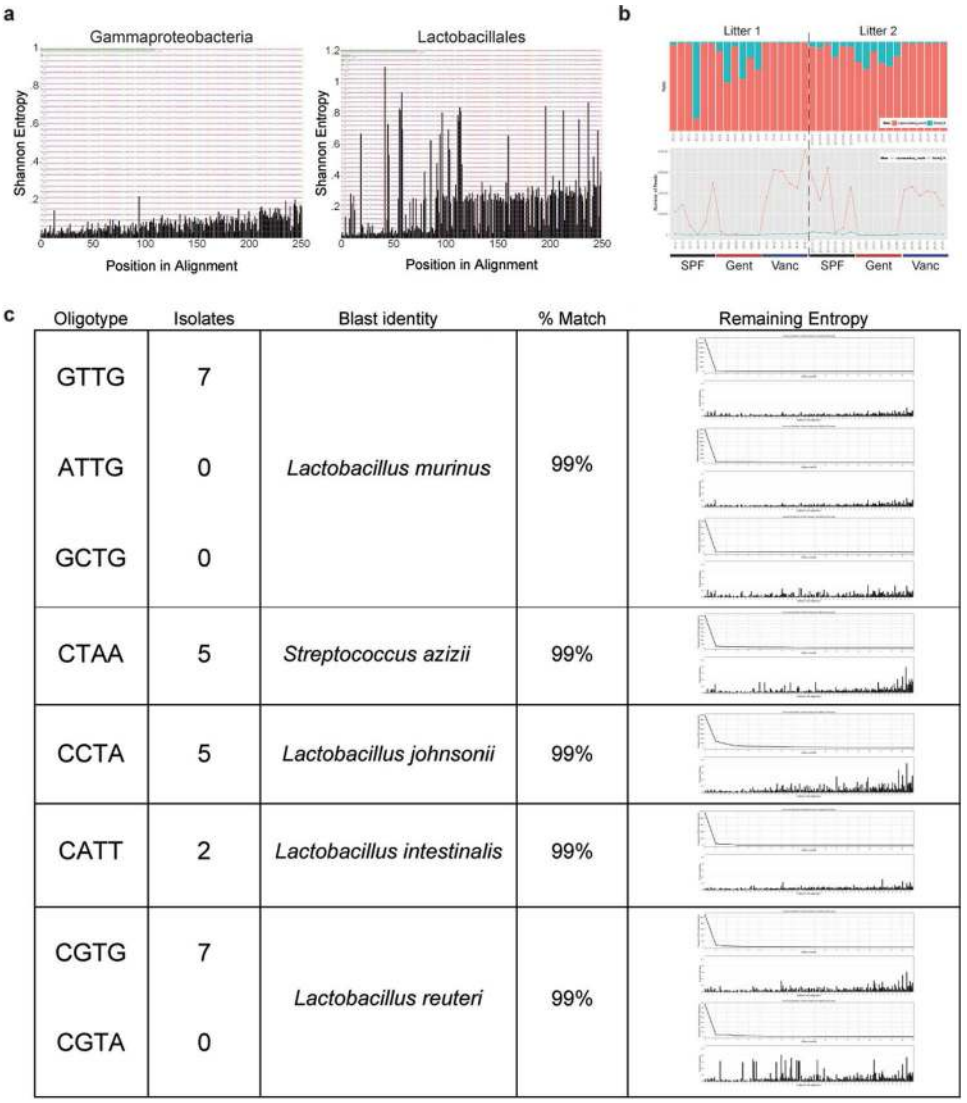

Extended Data Fig. 3 |. Perinatal antibiotics alter diversity of the intestinal microbiome.

(a) Initial Shannon entropy analysis of reads classified to Gammapreoteobacteria (left) or Lactobacillales (right). Oligotyping analysis was performed to resolve Lactobacillales oligotypes, but not carried out on Gammaproteobacteria reads due to low entropy. Shannon entropy by nucleotide position was calculated from the combined sequencing data described in Fig. 3e using the standard oligotyping pipeline. (b) Ratio (top) and absolute counts (bottom) of Lactobacillales reads in each sample aligning to any of the 8 oligotypes compared with reads failing to align. 465,160 reads from 36 samples were input and 453,693 were used in the final analysis after quality filtering. (c) 26 isolates from P5 intestinal samples were identified via BLAST of full length 16S gene sequence. Sequences from the V4 region of each oligotype resolved from previous analysis were aligned to each isolate. Table shows the number of isolates with > 98% match to a previously identified oligotype and the Shannon entropy measurements following oligotyping to highlight any unresolved diversity.

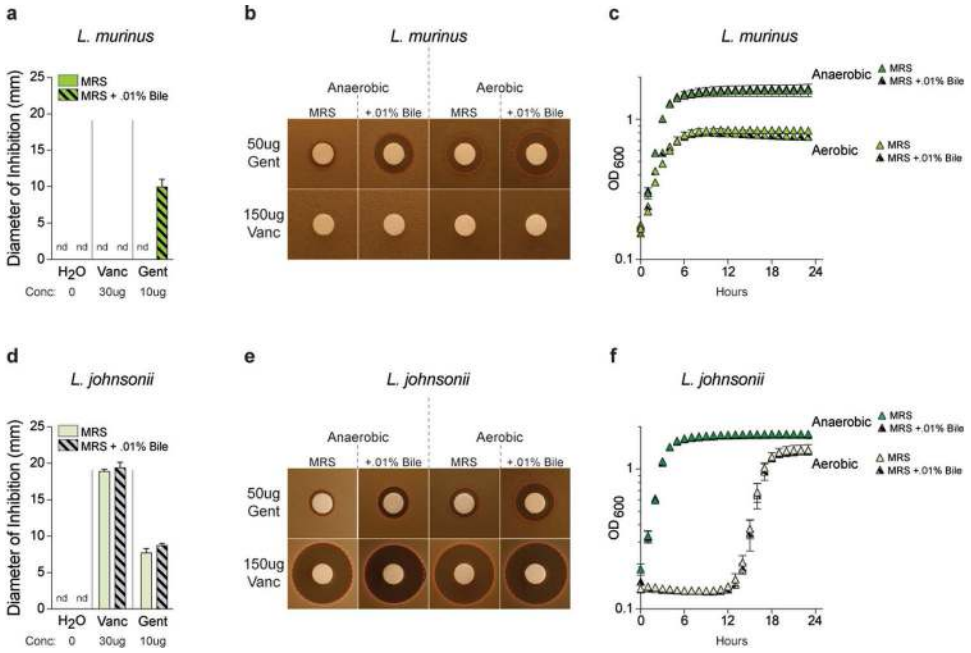

Extended Data Fig. 4 |. Lactobacilli species have divergent antibiotic resistance partially mediated by presence of bile acids.

Growth inhibition disk diffusion assay showing antibiotic susceptibility of endogenous isolates of L. murinus V10 (a,b) and L. johnsonii G2A (d,e) to vancomycin or gentamicin grown under aerobic or anaerobic conditions and with or without the addition of bile acids. Bars display mean ± SD. Growth curves of L. murinus (c) and L. johnsonii (f) under aerobic or anaerobic conditions and with or without the addition of bile acids (mean ± SD). No inhibition detected, nd. (a,d) Data are representative of 3 similar experiments; n = 3 plates per condition tested. (b,e) Data representative of 2 independent experiments; n = 3 plates per condition. (c,f) Data representative of 2 or 3 independent experiments; n = 3 wells per condition.

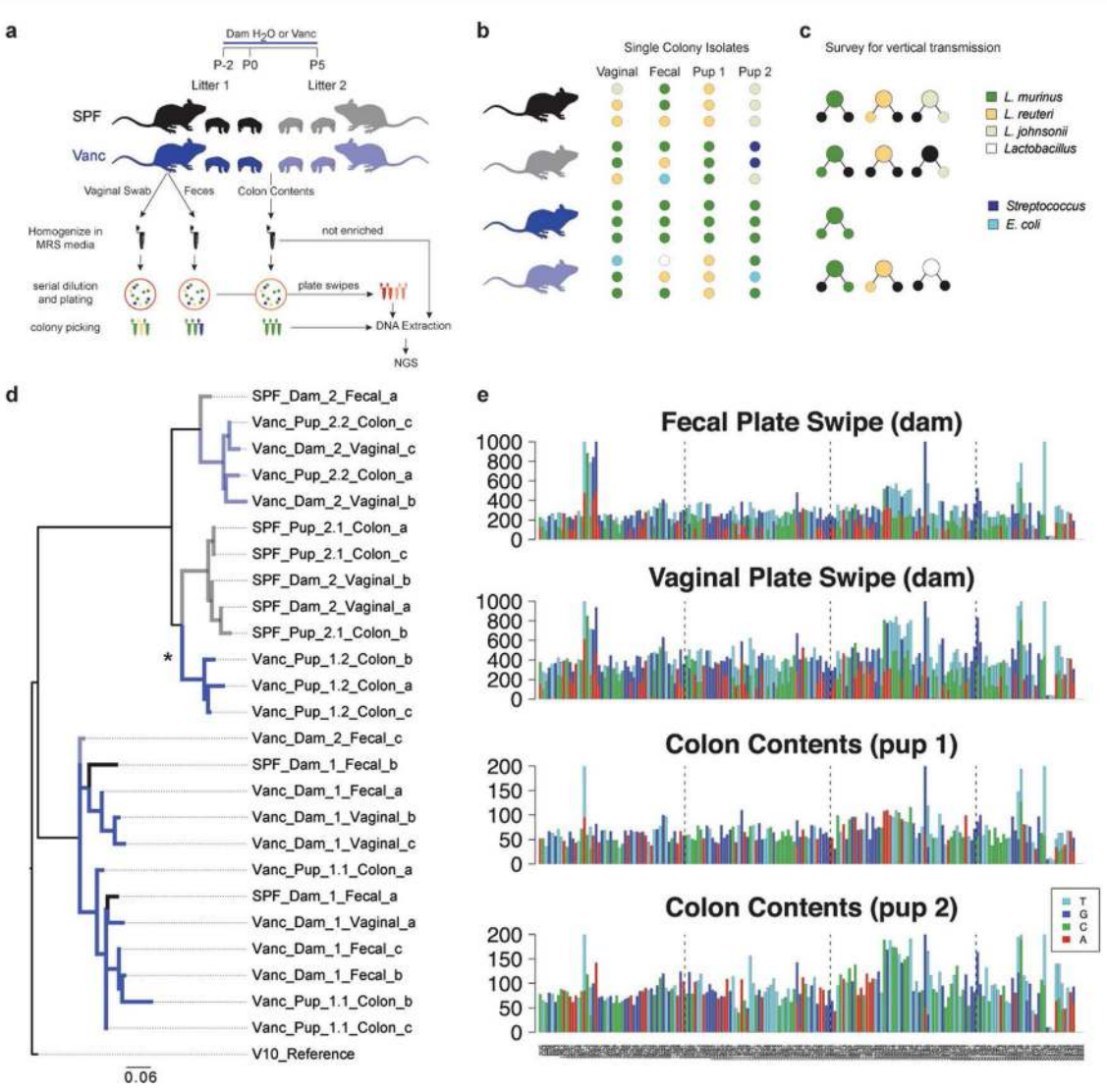

Extended Data Fig. 5 |. Vertical transmission of L. murinus in Vanc-reared litters.

(a) Experimental design. Littermate dams were separated 1 or 2 days prior to birth and drinking water was supplemented with vancomycin (Vanc) or left unchanged (SPF) until P5. SPF in black and Vanc in blue. Pup colon contents, maternal vaginal swabs, and fecal samples were homogenized in MRS and plated for single colony isolation of lactobacilli. DNA was simultaneously extracted from unenriched colon contents and 'plate swipes' after colony picking and subjected to shotgun metagenomics sequencing. (b) Taxonomic classification and (c) possible routes of vertical transmission based on colony isolates from dam and pup samples. Large circles represent the presence of maternal Lactobacillus isolate for given taxonomy. Small circles represent the presence of pup isolate. Black circles indicate that no isolates were identified from the sample. Data are from 2 pups per litter in 2 litters of either SPF or Vanc-reared pups and their dam. (d) A phylogenetic tree built from core SNPs from 26 L. murinus isolate genomes. The V10 isolate was selected as the reference. The branches of the tree associated with each litter/dam share the same color. The starred clade (*) is composed of isolates from a single pup that do not cluster with the

associated dam. Phylogenetic relationships between all 26 L. murinus isolates identified in this study based on 187 core SNPs were used. (e) Observed allele read counts for 187 core SNPs. Each bar shows the number of metagenomic reads aligned to that position in the reference. Bars are colored to show the relative abundance of each base at that position. Allele frequencies of 187 core SNPs from plate-swabs of fecal and vaginal lactobacilli of a single vanc dam and colon contents of her pups.

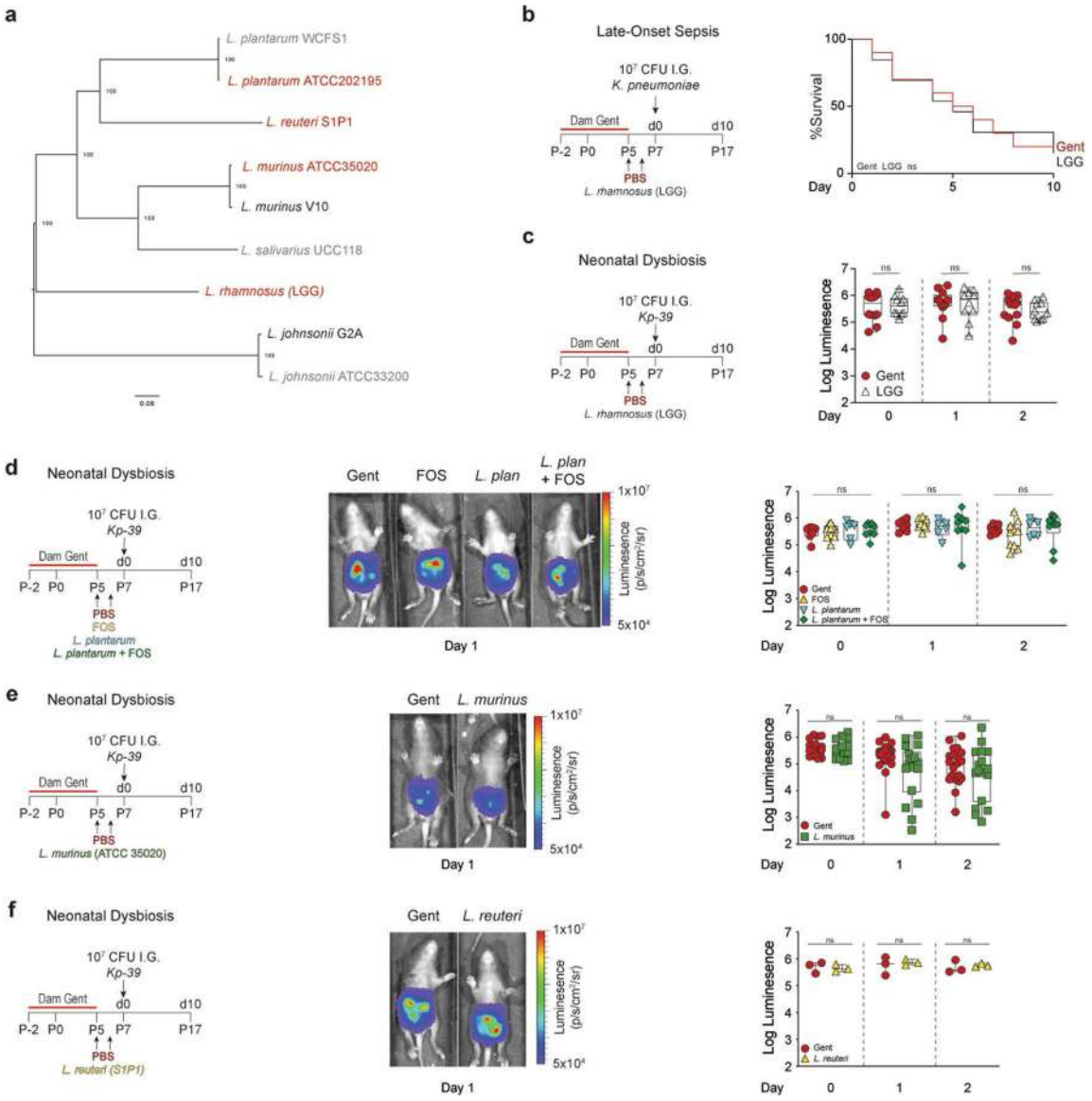

Extended Data Fig. 6 |. Protective probiosis of lactobacilli is not generalizable across species and strains.

(a) A phylogenetic tree constructed from 259 single copy genes with shared homology across all genomes using 'Codon Tree' protocol of PATRIC's Phylogentic Tree building service. Colors indicate whether strains protect (black) or do not protect (red) against neonatal dysbiosis. Reference strains not used in the study are in gray. Gent pups received PBS or probiotic Lactobacillus rhamnosus GG (LGG) i.g prior to infection with 107 CFU Kp-43816lux (b) or (c) and monitored daily for sepsis (curve) or abdominal bioluminescence, respectively. Pooled from 2 independent experiments using within-litter controls: Gent (n = 10); LGG (n = 13) (b), or pooled from 3 separate cages of within-litter controls in a single infection experiment: Gent (n = 12); LGG (n = 10) (c). (d) Gent pups received PBS, fructooligosaccharide (FOS), L. plantarum (), or FOS and L. plantarum i.g. prior to infection with 107 CFU Kp-39lux. Pooled from 4 independent experiments using within-litter controls: Gent (n = 12); Fructooligosaccharide (n = 13); L. plantarum (n = 10),

L. plantarum and fructooligosaccharide (n = 13). (e) Gent pups received PBS or L. murinus (ATCC 35020) i.g. prior to infection with 107 CFU Kp-39lux. Pooled from 3 independent experiments from 4 litters with within-litter controls: Gent (n = 21); L. murinus (n = 18). (f) Gent pups received PBS or L. reuteri (S1P1) i.g. prior to infection with 107 CFU Kp-39lux. Representative abdominal bioluminescence is shown and quantitated. Box and whisker plots show median and IQR with lines extending as the 1st and 4th quartile. Data are representative of 2 independent experiments: Gent (n = 3); L. reuteri (n = 3). Number of pups of either sex, n.

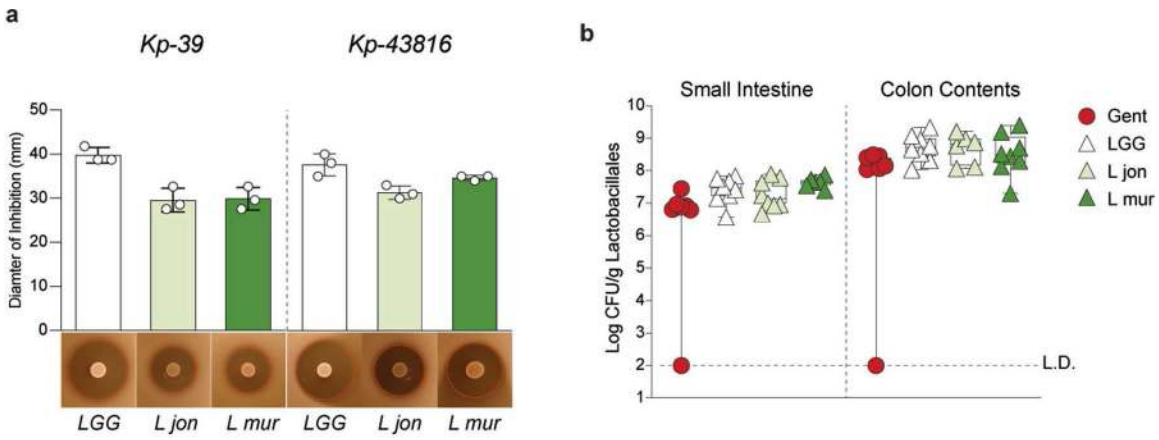

Extended Data Fig. 7 |. Probiotic activity of lactobacilli does not correlate with in vitro growth inhibition or in vivo engraftment.

(a) Growth inhibition colony diffusion assay showing ability of lactobacilli to directly inhibit growth of Kp-39 (left) or Kp-43816 (right). Bars display mean ± SD. Data are representative of 2 independent experiments; n = 3 plates per condition tested. (b) Lactobacilli CFU from small intestine or colon contents of P7 littermates reared with gentamicin and given 50 µl PBS, L. murinus V10, LGG, or L. johnsonii G2A, i.g on P5 and P6. Box and whisker plots show median and IQR with lines extending as the 1st and 4th quartile. Pooled from 2 independent experiments: Gent (n = 7); L. murinus (n = 8); LGG (n = 8); L. johnsonii (n = 6). Number of pups of either sex, n.

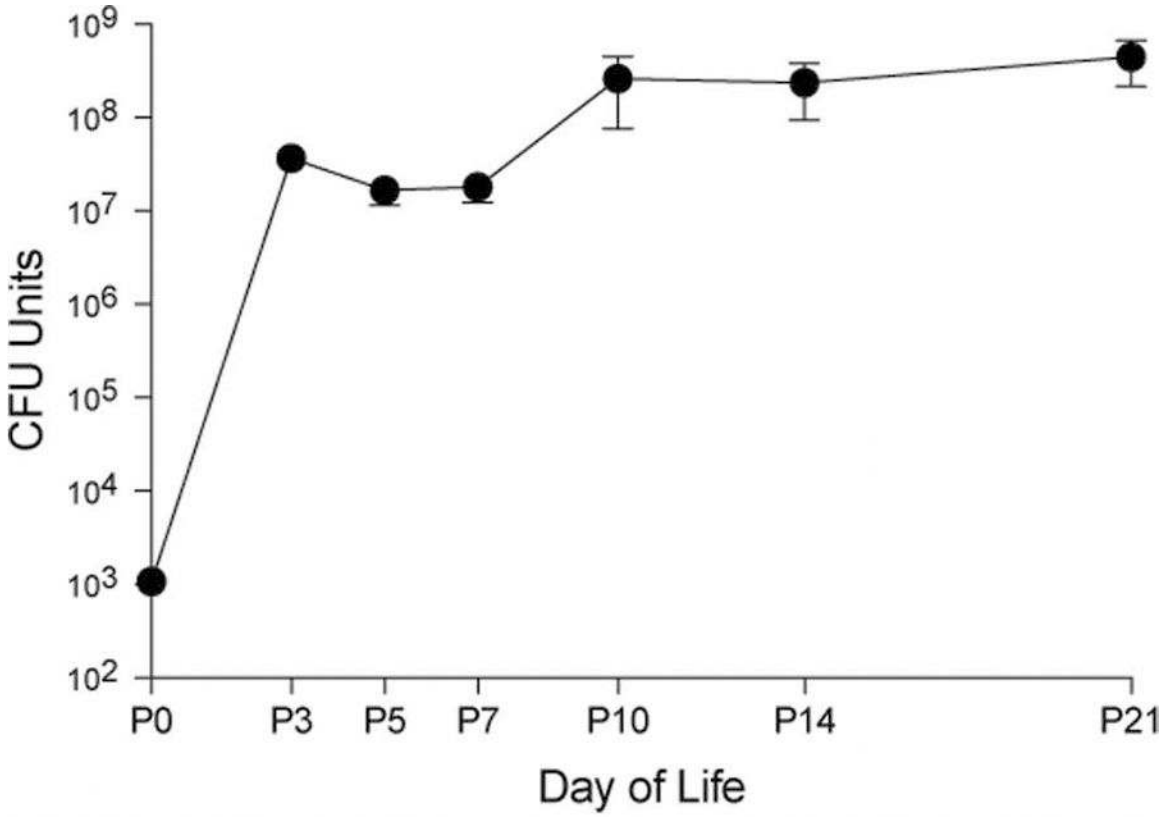

Extended Data Fig. 8 |. Microbiome abundance during primary succession.

DNA was extracted from intestinal tissue at indicated days from birth to weaning and bacterial abundance was measured by qPCR of 16S rRNA gene (mean ± SE). Data are from a single experiment: P0 (n = 3); P3 (n = 5); P5 (n = 5); P7 (n = 5); P10 (n = 5); P14 (n = 5); P21 (n = 5). Number of pups of either sex, n.

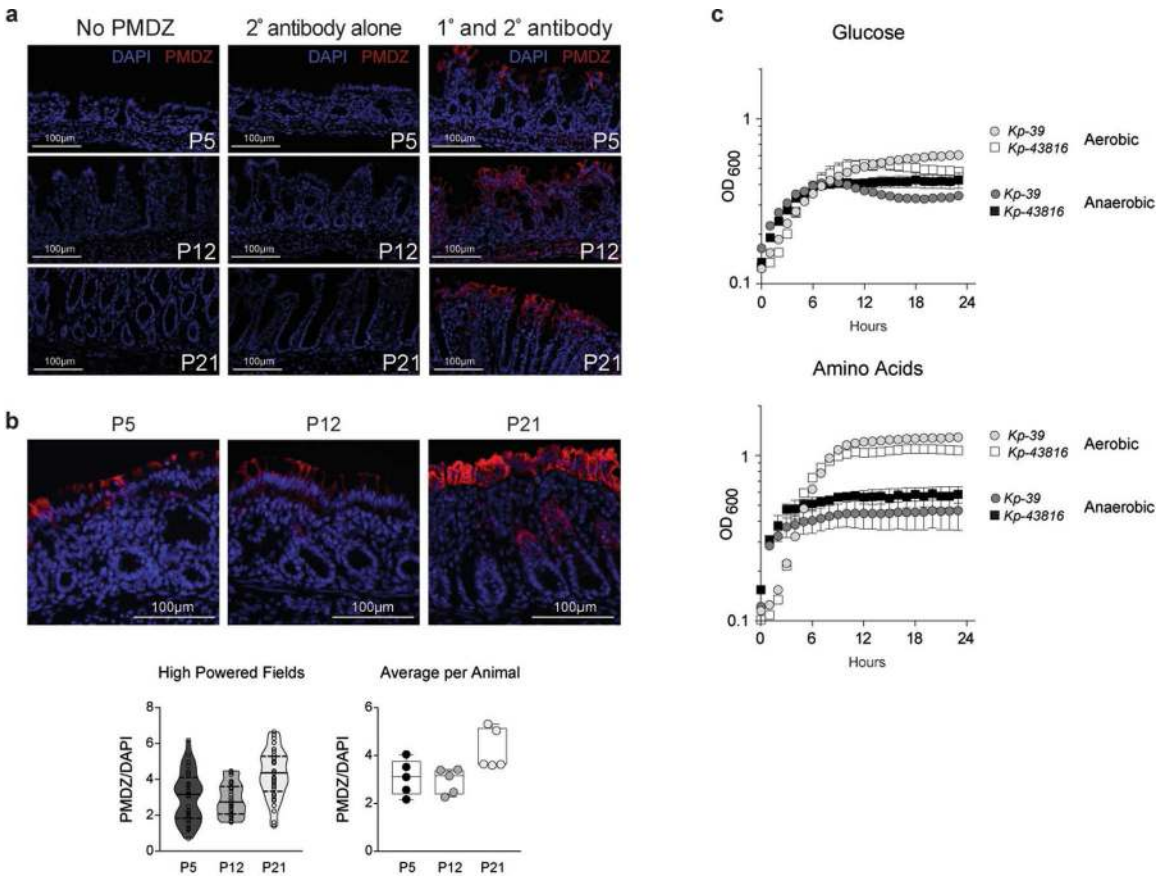

Extended Data Fig. 9 |. The aerobic neonatal intestine supports rapid *K. pneumoniae* expansion. (a) Representative images validating the specificity of hypoxyprobe staining across all ages assayed (P5, P12, and P21). Non-specific staining is not observed with secondary antibody alone or when PMDZ is withheld from administration. Images are representative of controls used in every experiment using PMDZ hypoxyprobe assay. (b) Representative images of hypoxyprobe assay measuring ratio of PMDZ adducts (red) to DAPI (blue) from randomly selected sections of mid-distal colon in pups at different ages prior to weaning (upper panel). Average intensity of all fields (left) and average intensity per mouse (right) are displayed (lower panel). Violin plots show median (solid line) and quartiles (dashed line) of all measurements. Data are representative of 2 independent experiments; n = 5 animals per age. (c) Growth curves of *K. pneumoniae* in minimal media under aerobic or anaerobic conditions with either glucose (left) or amino acids (right) as a sole carbon source (mean ± SD). Data are representative of 3 independent experiments; n = 3 wells per condition.

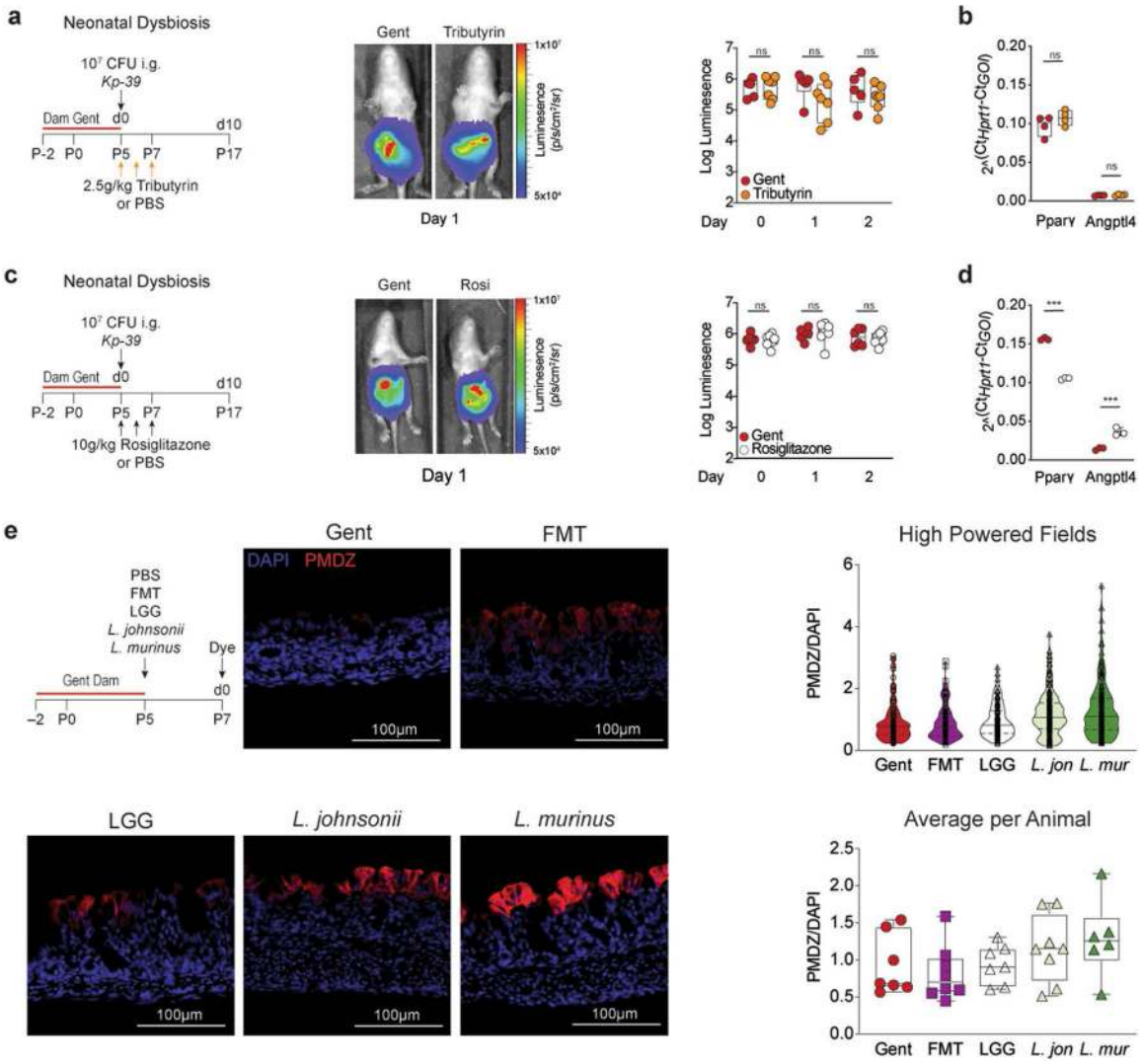

Extended Data Fig. 10 |. Neither butyrate nor PPARg activation protect against neonatal dysbiosis.

(a) (b) Gent pups received PBS or tributyrin i.g. for 3 days following infection with 107 CFU. Abdominal bioluminescence was measured daily. Pooled from 2 independent experiments using within-litter controls (a): Gent (n = 7); Tributyrin (n = 8). Representative of 2 independent experiments using within-litter controls (b); n = 4 mice per group. (c,d) Gene expression of Pparg and Angptl4 in colon of uninfected P7 gent pups receiving 3 days treatment with PBS or tributyrin. (c) Gent pups received PBS or PPARg agonist rosiglitazone i.g. for 3 days following infection with 107 CFU Kp-39lux. Abdominal bioluminescence was measured daily. Pooled from 2 independent experiments using within-litter controls: Gent (n = 6), Rosiglitazone (n = 7). (d) Gene expression of Pparg and Angptl4 in colon of uninfected P7 gent pups receiving 3 days treatment with PBS or rosiglitazone. Box and whisker plots show median and IQR with lines extending as the 1st and 4th quartile. Data are representative of 2 independent experiments using controls; n = 3 mice per group. (e) Representative images of hypoxyprobe assay measuring ratio of PMDZ adducts (red) to DAPI (blue) from randomly selected sections of mid-distal colon in P7

littermates reared with gentamicin and given 50 μl PBS (Gent), fecal microbiome transplant (FMT), L. rhamnosus GG (LGG), L. johnsonii G2A, or L. murinus V10 i.g on P5 and P6. Average intensity of all high-powered fields (top) and average intensity per mouse (bottom) are displayed. Violin plots show median (solid line) and quartiles (dashed line) of all measurements. Pooled from 2 independent experiments: Gent (n = 7); FMT (n = 8); LGG (n = 7); L. johnsonii (n = 8); L. murinus (n = 6). Number of pups of either sex, n.

Supplementary Material

Refer to Web version on PubMed Central for supplementary material.

Acknowledgements

We thank members of the Weaver laboratory for their helpful comments, G. Gaskins and C. Rutledge for their administrative support and S.E. Winter (UT Southwestern), N. Ambalavanan, C.O. Elson III, R.G. Lorenz, R.D. Hatton and L.A. Harrington (UAB) for their advice. We thank M. Wu (University of North Dakota), G. O'Toole (Dartmouth University) and C. Orihuela (UAB) for providing critical reagents to this study (Supplementary Tables 3 and 4). We also thank D. O'Quinn, J. Wright and H. Turner for their technical assistance. Additionally, we are grateful to T. Schaub and S. Sinclair at the UAB Gnotobiotic Animal Core, S. Samuel and K. Zinn at the UAB Small Animal Imaging Core, and J. Day and the La Jolla Institute of Allergy and Immunology Sequencing Facility. Finally, we thank W. Duck and P. Basu Thakur for their advice and technical assistance and P. Thomas and M. Park for bioinformatics analysis. We acknowledge the following for their support of the Microbiome Resource at the University of Alabama at Birmingham: the Comprehensive Cancer Center (P30AR050948), the Center for Clinical Translational Science (UL1TR001417) and the University-Wide Institutional Core and Heflin Center for Genomic Sciences. This study used the Nephele platform from the National Institute of Allergy and Infectious Diseases Office of Cyber Infrastructure and Computational Biology in Bethesda and utilized the high-performance computational capabilities of the National Institutes of Health (NIH) Biowulf Linux cluster. Wholegenome sequencing was performed at the NIH Intramural Sequencing Center. This work was supported by NIH F30DK105680 (J.R.S.), the UAB Medical Scientist Training Program, supported by NIH T32GM008361 (E.G.B., D.D., V.A.L. and J.R.S.), NHGRI Intramural Research funds (J.A.S.) and UAB institutional funds (C.T.W. and D.A.R.).

References

1. Liu L et al. Global, regional, and national causes of child mortality in 2000–13, with projections to inform post-2015 priorities: an updated systematic analysis. Lancet 385, 430–440 (2015). [PubMed: 25280870]
2. Stoll BJ et al. Trends in care practices, morbidity, and mortality of extremely preterm neonates, 1993–2012. JAMA 314, 1039–1051 (2015). [PubMed: 26348753]
3. Dong Y & Speer CP Late-onset neonatal sepsis: recent developments. Arch. Dis. Child. Fetal Neonatal Ed 100, F257–F263 (2015). [PubMed: 25425653]
4. Kuppala V, Meinzen-Derr J & Morrow A Prolonged initial empirical antibiotic treatment is associated with adverse outcomes in premature infants. J. Pediatr 159, 720–725 (2011). [PubMed: 21784435]
5. Fajardo C, Alshaikh B & Harabor A Prolonged use of antibiotics after birth is associated with increased morbidity in preterm infants with negative cultures. J. Matern. Fetal Neonatal Med 64, 1–7 (2018).
6. Gibson MK et al. Developmental dynamics of the preterm infant gut microbiota and antibiotic resistome. Nat. Microbiol 1, 16024 (2016). [PubMed: 27572443]
7. Yassour M et al. Natural history of the infant gut microbiome and impact of antibiotic treatment on bacterial strain diversity and stability. Sci. Transl. Med 8, 343ra81 (2016).
8. Parm Ü, Metsvaht T, Ilmoja M-L & Lutsar I Gut colonization by aerobic microorganisms is associated with route and type of nutrition in premature neonates. Nutr. Res 35, 496–503 (2015). [PubMed: 25922115]

9. Bokulich NA et al. Antibiotics, birth mode, and diet shape microbiome maturation during early life. Sci. Transl. Med 8, 343ra82 (2016).
10. Korpela K et al. Intestinal microbiota development and gestational age in preterm neonates. Sci. Rep 8, 2453 (2018). [PubMed: 29410448]
11. Tarr PI & Warner BB Gut bacteria and late-onset neonatal bloodstream infections in preterm infants. Semin. Fetal Neonatal Med 21, 388–393 (2016). [PubMed: 27345372]
12. Graham PL, Della-Latta P, Wu F, Zhou J & Saiman L The gastrointestinal tract serves as the reservoir for Gram-negative pathogens in very low birth weight infants. Pediatr. Infect. Dis. J 26, 1153–1156 (2007). [PubMed: 18043457]
13. Knoop KA et al. Microbial antigen encounter during a preweaning interval is critical for tolerance to gut bacteria. Sci. Immunol 2, eaao1314 (2017). [PubMed: 29246946]
14. Kim Y-G et al. Neonatal acquisition of *Clostridia* species protects against colonization by bacterial pathogens. Science 356, 315–319 (2017). [PubMed: 28428425]
15. Tourneur E & Chassin C Neonatal immune adaptation of the gut and its role during infections. Clin. Dev. Immunol 2013, 270301–270317 (2013). [PubMed: 23737810]
16. Dermyshi E et al. The 'golden age' of probiotics: a systematic review and meta-analysis of randomized and observational studies in preterm infants. Neonatology 112, 9–23 (2017). [PubMed: 28196365]
17. van den Akker CHP et al. Probiotics for preterm infants: a strain-specific systematic review and network meta-analysis. J. Pediatr. Gastroenterol. Nutr 67, 103–122 (2018). [PubMed: 29384838]
18. Deshmukh HS et al. The microbiota regulates neutrophil homeostasis and host resistance to *Escherichia coli* K1 sepsis in neonatal mice. Nat. Med 20, 524–530 (2014). [PubMed: 24747744]
19. Ulas T et al. S100-alarmin-induced innate immune programming protects newborn infants from sepsis. Nat. Immunol 18, 622–632 (2017). [PubMed: 28459433]
20. Howe K et al. Development of stable reporter system cloning *luxCDABE* genes into chromosome of *Salmonella enterica* serotypes using Tn7 transposon. BMC Microbiol 10, 197 (2010). [PubMed: 20653968]
21. Langstraat J, Bohse M & Clegg S Type 3 fimbrial shaft (MrkA) of Klebsiella pneumoniae, but not the fimbrial adhesin (MrkD), facilitates biofilm formation. Infect. Immun 69, 5805–5812 (2001). [PubMed: 11500458]
22. Ko KS The contribution of capsule polysaccharide genes to virulence of Klebsiella pneumoniae. Virulence 8, 485–486 (2017). [PubMed: 27715471]
23. Pamer EG Resurrecting the intestinal microbiota to combat antibiotic-resistant pathogens. Science 352, 535–538 (2016). [PubMed: 27126035]
24. Patel S & Bernice F Vancomycin in StatPearls https://www.ncbi.nlm.nih.gov/pubmed/29083794 (StatPearls Publishing, 2018).
25. Miranda JC et al. Gentamicin absorption during prophylactic use for necrotizing enterocolitis. Dev. Pharmacol. Ther 7, 303–306 (1984). [PubMed: 6478984]
26. Milani C et al. Phylotype-level profiling of lactobacilli in highly complex environments by means of an internal transcribed spacer-based metagenomics approach. Appl. Environ. Microbiol 84, e00706–e00718 (2018). [PubMed: 29728382]
27. Eren AM et al. Oligotyping: differentiating between closely related microbial taxa using 16S rRNA gene data. Methods Ecol. Evol 4, 1111–1119 (2013).
28. Ammor MS, Belén Flórez A & Mayo B Antibiotic resistance in non-enterococcal lactic acid bacteria and bifidobacteria. Food Microbiol 24, 559–570 (2007). [PubMed: 17418306]
29. Elkins CA & Mullis LB Bile-mediated aminoglycoside sensitivity in *Lactobacillus* species likely results from increased membrane permeability attributable to cholic acid. Appl. Environ. Microbiol 70, 7200–7209 (2004). [PubMed: 15574918]
30. Yassour M et al. Strain-level analysis of mother-to-child bacterial transmission during the first few months of life. Cell Host Microbe 24, 146–154 (2018). [PubMed: 30001517]
31. Ferretti P et al. Mother-to-infant microbial transmission from different body sites shapes the developing infant gut microbiome. Cell Host Microbe 24, 133–145 (2018). [PubMed: 30001516]

32. Taft DH et al. Center variation in intestinal microbiota prior to late-onset sepsis in preterm infants. PloS One 10, e0130604 (2015). [PubMed: 26110908]
33. Madan JC et al. Gut microbial colonisation in premature neonates predicts neonatal sepsis. Arch. Dis. Child. Fetal Neonatal Ed 97, F456–F462 (2012). [PubMed: 22562869]
34. Mai V et al. Distortions in development of intestinal microbiota associated with late onset sepsis in preterm infants. PloS One 8, e52876 (2013). [PubMed: 23341915]
35. Litvak Y, Byndloss MX & Baumler AJ Colonocyte metabolism shapes the gut microbiota. Science 362, eaat9076 (2018). [PubMed: 30498100]
36. Rivera-Chávez F et al. Depletion of butyrate-producing *Clostridia* from the gut microbiota drives an aerobic luminal expansion of *Salmonella*. Cell Host Microbe 19, 443–454 (2016). [PubMed: 27078066]
37. Cramton SE, Ulrich M, Götz F & Döring G Anaerobic conditions induce expression of polysaccharide intercellular adhesin in *Staphylococcus aureus* and *Staphylococcus epidermidis*. Infect. Immun 69, 4079–4085 (2001). [PubMed: 11349079]
38. Byndloss MX & Baumler AJ The germ-organ theory of non-communicable diseases. Nat. Rev. Microbiol 16, 103–110 (2018). [PubMed: 29307890]
39. Lodinová-Zádniková R & Sonnenborn U Effect of preventive administration of a nonpathogenic Escherichia coli strain on the colonization of the intestine with microbial pathogens in newborn infants. Biol. Neonate 71, 224–232 (1997). [PubMed: 9129791]
40. Birchenough GMH et al. Altered innate defenses in the neonatal gastrointestinal tract in response to colonization by neuropathogenic *Escherichia coli*. Infect. Immun 81, 3264–3275 (2013). [PubMed: 23798529]
41. Grozdanov L et al. Analysis of the genome structure of the nonpathogenic probiotic *Escherichia coli* strain Nissle 1917. J. Bacteriol 186, 5432–5441 (2004). [PubMed: 15292145]
42. Reed BD, Schibler KR, Deshmukh H, Ambalavanan N & Morrow AL The impact of maternal antibiotics on neonatal disease. J. Pediatr 197, 97–103 (2018). [PubMed: 29551319]
43. Schulman J et al. Neonatal intensive care unit antibiotic use. Pediatrics 135, 826–833 (2015). [PubMed: 25896845]
44. Rao SC, Athalye-Jape GK, Deshpande GC, Simmer KN & Patole SK Probiotic supplementation and late-onset sepsis in preterm infants: a meta-analysis. Pediatrics 137, e20153684 (2016). [PubMed: 26908700]
45. Viswanathan S, Lau C, Akbari H, Hoyen C & Walsh MC Survey and evidence-based review of probiotics used in very low birth weight preterm infants within the United States. J. Perinatol 36, 1106–1111 (2016). [PubMed: 27583387]
46. Suez J, Zmora N, Segal E & Elinav E The pros, cons, and many unknowns of probiotics. Nat. Med 25, 716–729 (2019). [PubMed: 31061539]
47. Segers ME & Lebeer S Towards a better understanding of *Lactobacillus rhamnosus* GG–host interactions. Microb. Cell Fact 13, S7 (2014). [PubMed: 25186587]
48. Panigrahi P et al. A randomized synbiotic trial to prevent sepsis among infants in rural India. Nature 548, 407–412 (2017). [PubMed: 28813414]
49. Kelly CJ et al. Crosstalk between microbiota-derived short-chain fatty acids and intestinal epithelial HIF augments tissue barrier function. Cell Host Microbe 17, 662–671 (2015). [PubMed: 25865369]
50. Byndloss MX et al. Microbiota-activated PPAR-γ signaling inhibits dysbiotic Enterobacteriaceae expansion. Science 357, 570–575 (2017). [PubMed: 28798125]
51. Lee A & Gemmell E Changes in the mouse intestinal microflora during weaning: role of volatile fatty acids. Infect. Immun 5, 1–7 (1972). [PubMed: 4656353]
52. Hosny M, Cassir N & La Scola B Updating on gut microbiota and its relationship with the occurrence of necrotizing enterocolitis. Hum. Microbiome J 4, 14–19 (2017).
53. Corsini I et al. Peroxisome proliferator-activated receptor-γ agonist pioglitazone reduces the development of necrotizing enterocolitis in a neonatal preterm rat model. Pediatr. Res 81, 364–368 (2017). [PubMed: 27973471]

54. Friedman ES et al. Microbes versus chemistry in the origin of the anaerobic gut lumen. Proc. Natl Acad. Sci. USA 115, 4170–4175 (2018). [PubMed: 29610310]
55. de Goffau MC et al. Human placenta has no microbiome but can contain potential pathogens. Nature 572, 329–334 (2019). [PubMed: 31367035]
56. Pedersen MB, Gaudu P, Lechardeur D, Petit M-A & Gruss A Aerobic respiration metabolism in lactic acid bacteria and uses in biotechnology. Annu. Rev. Food Sci. Technol 3, 37–58 (2012). [PubMed: 22385163]
57. Wilck N et al. Salt-responsive gut commensal modulates T_H17 axis and disease. Nature 551, 585–589 (2017). [PubMed: 29143823]
58. Singh AK, Hertzberger RY & Knaus UG Hydrogen peroxide production by lactobacilli promotes epithelial restitution during colitis. Redox Biol 16, 11–20 (2018). [PubMed: 29471162]
59. Lee Y-S et al. Microbiota-derived lactate accelerates intestinal stem-cell-mediated epithelial development. Cell Host Microbe 24, 833–846 (2018). [PubMed: 30543778]
60. Litvak Y et al. Commensal Enterobacteriaceae protect against *Salmonella* colonization through oxygen competition. Cell Host Microbe 25, 128–139 (2019). [PubMed: 30629913]

References

61. Hinsa SM, Espinosa-Urgel M, Ramos JL & O'Toole GA Transition from reversible to irreversible attachment during biofilm formation by *Pseudomonas fluorescens* WCS365 requires an ABC transporter and a large secreted protein. Mol. Microbiol 49, 905–918 (2003). [PubMed: 12890017]
62. McKenzie GJ & Craig NL Fast, easy and efficient: site-specific insertion of transgenes into enterobacterial chromosomes using Tn7 without need for selection of the insertion event. BMC Microbiol 6, 39 (2006). [PubMed: 16646962]
63. Kumar R et al. Getting started with microbiome analysis: sample acquisition to bioinformatics. Curr. Protoc. Hum. Genet 82, 18.8.1–18.8.29 (2014). [PubMed: 25042718]
64. Segata N et al. Metagenomic biomarker discovery and explanation. Genome Biol 12, R60 (2011). [PubMed: 21702898]
65. Meadow J q2oligo—convert QIIME files into oligotyping subsets. GitHub https://github.com/jfmeadow/q2oligo (2014).
66. Bergey DH Bergey's Manual of Systematics of Archaea and Bacteria Bergey's Manual Trust 10.1002/9781118960608 (2015).
67. Ormerod KL et al. Genomic characterization of the uncultured Bacteroidales family S24–7 inhabiting the guts of homeothermic animals. Microbiome 4, 36 (2016). [PubMed: 27388460]
68. Tegtmeier D, Riese C, Geissinger O, Radek R & Brune A *Breznakia blatticola* gen. nov. sp. nov. and *Breznakia pachnodae* sp. nov., two fermenting bacteria isolated from insect guts, and emended description of the family Erysipelotrichaceae. Syst. Appl. Microbiol 39, 319–329 (2016). [PubMed: 27270136]
69. Weingarten RA et al. Genomic analysis of hospital plumbing reveals diverse reservoir of bacterial plasmids conferring carbapenem resistance. mBio 9, e02011–e02017 (2018). [PubMed: 29437920]
70. Nurk S et al. Assembling single-cell genomes and mini-metagenomes from chimeric MDA products. J. Comput. Biol 20, 714–737 (2013). [PubMed: 24093227]
71. Koren S et al. Canu: scalable and accurate long-read assembly via adaptive *k*-mer weighting and repeat separation. Genome Res 27, 722–736 (2017). [PubMed: 28298431]
72. Treangen TJ, Ondov BD, Koren S & Phillippy AM The harvest suite for rapid core-genome alignment and visualization of thousands of intraspecific microbial genomes. Genome Biol 15, 524 (2014). [PubMed: 25410596]
73. Wyres KL et al. Identification of *Klebsiella* capsule synthesis loci from whole genome data. Microb. Genomics 2, 1–15 (2016).
74. Johnson RC et al. Investigation of a cluster of *Sphingomonas koreensis* infections. N. Engl. J. Med 379, 2529–2539 (2018). [PubMed: 30586509]
75. Wood DE & Salzberg SL Kraken: ultrafast metagenomic sequence classification using exact alignments. Genome Biol 15, R46 (2014). [PubMed: 24580807]

76. Langmead B & Salzberg SL Fast gapped-read alignment with Bowtie 2. Nat. Meth 9, 357–359 (2012).

77. Bates D, Mächler M, Bolker B & Walker S Fitting linear mixed-effects models using lme4. J. Stat. Software 1, 1–48 (2015).

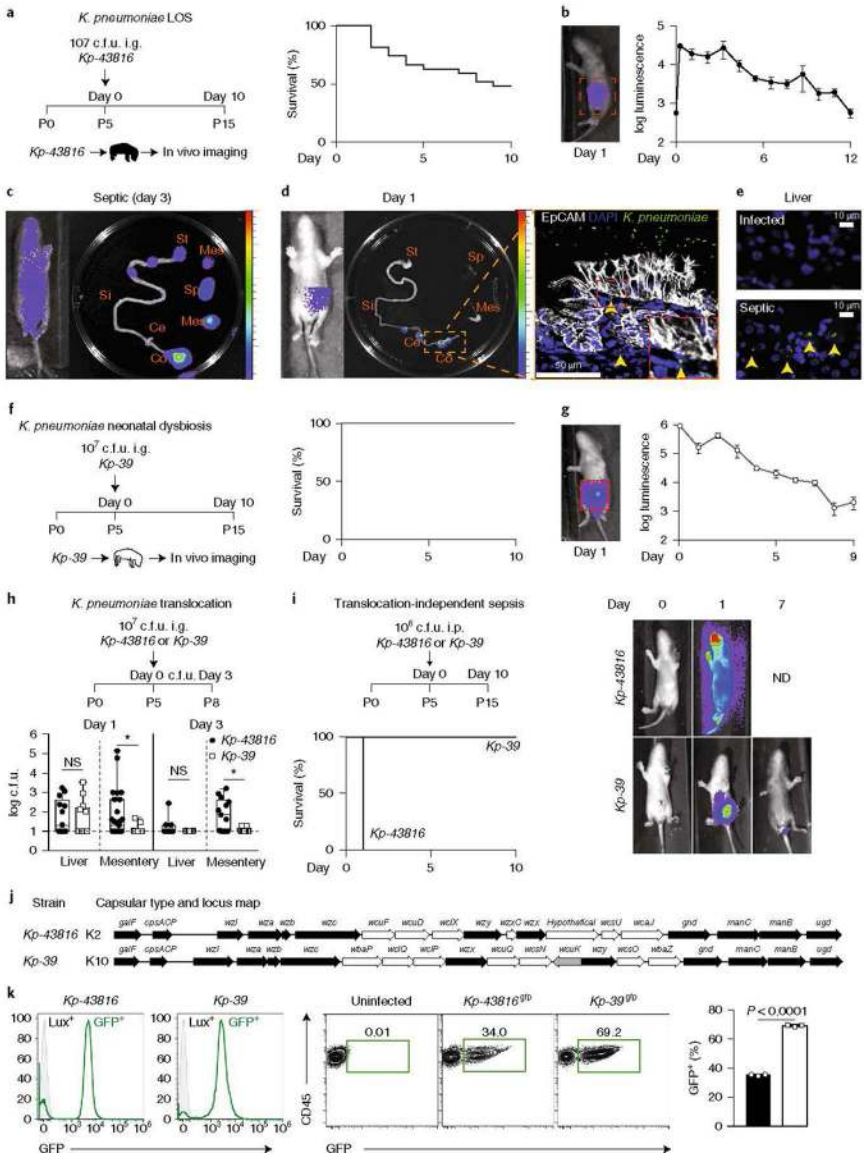

Fig. 1 |. Neonatal dysbiosis becomes LOS when *K. pneumoniae* are not cleared following translocation.

a,**b**, Schematic illustration for the LOS model. Litters of pups ($n = 6$–12 pups of either sex) were infected i.g. with 10^7 c.f.u. *Kp-43816*^{lux} at day 5 of life (P5) and monitored daily for sepsis (**a**) (Kaplan–Meier curve) and abdominal bioluminescence (**b**) (log10-transformed mean ± s.e.m.). $n = 27$ pups pooled from three independent experiments. **c**, Representative image of a pup with LOS (left) and ex vivo organ imaging (right). St, stomach; Si, small intestine; Ce, cecum; Co, colon; Mes, mesentery; Sp, spleen. **d**, Pups were infected with 5×10^6 c.f.u. *Kp-43816*^{lux} and 5×10^6 c.f.u. *Kp-43816*^{gfp}. At 24 h after infection, colonic tissue was fixed, frozen and cryosectioned from nonseptic pups. Translocation was assessed using confocal microscopy to determine where *Kp-43816*^{gfp} (green) crossed the epithelial barrier, stained with anti-EpCAM (white). Tissue was counterstained with DAPI (blue). Yellow arrowheads indicate translocated *K. pneumoniae*. **e**, Representative liver sections stained with DAPI (blue) from nonseptic (top) and septic (bottom) pups 3 d after infection with 10^7

Kp-43816^{gfp} (green). **f**,**g**, Schematic illustration of neonatal dysbiosis model. Litters of pups (n = 6–12) were infected i.g. with 10^7 c.f.u. *Kp-39*^{lux} at day 5 of life (P5) and monitored daily for sepsis (**f**) (Kaplan–Meier curve) and abdominal bioluminescence (**g**) (log_{10}-transformed mean ± s.e.m.). n = 8 pups from one litter. Data are representative of three independent experiments. **h**, c.f.u. of translocated *K. pneumoniae* recovered from the liver and mesentery of nonseptic pups 1 d (left) or 3 d (right) after infection. Box-and-whisker plots show the median and interquartile range (IQR), with lines extending to the first and fourth quartiles. Each point represents an organ from an infected pup. Day 1: *Kp-43816* liver, n = 13; *Kp-43816* mesentery, n = 27; *Kp-39* liver, n = 13; and *Kp-39* mesentery, n = 17; day 3: *Kp-43816* liver, n = 8; *Kp-43816* mesentery, n = 13;, *Kp-39* liver, n = 9; and *Kp-39* mesentery, n = 9. Data were pooled from four independent experiments. NS, not significant. **i**, *Kp-43816*^{lux} or *Kp-39*^{lux} (10^6 c.f.u.) were given i.p. to P5 pups and pups were monitored daily for survival (Kaplan–Meier curve) and evidence of sepsis. n = 5 pups per group; data are representative of three independent experiments. ND, not detected. **j**, Capsule locus maps and molecular capsule typing analysis on both strains of *K. pneumoniae*. n = 3 wells per group; data are representative of four independent experiments. **k**, Fluorescence signal of reporter strains of *K. pneumoniae* (left) and GFP fluorescence intensity (mean ± s.d.) of J774A.1 macrophages either uninfected or infected with GFP$^+$ *K. pneumoniae* (right). In all instances, n refers to the number of pups of either sex. *P ≤0.05.

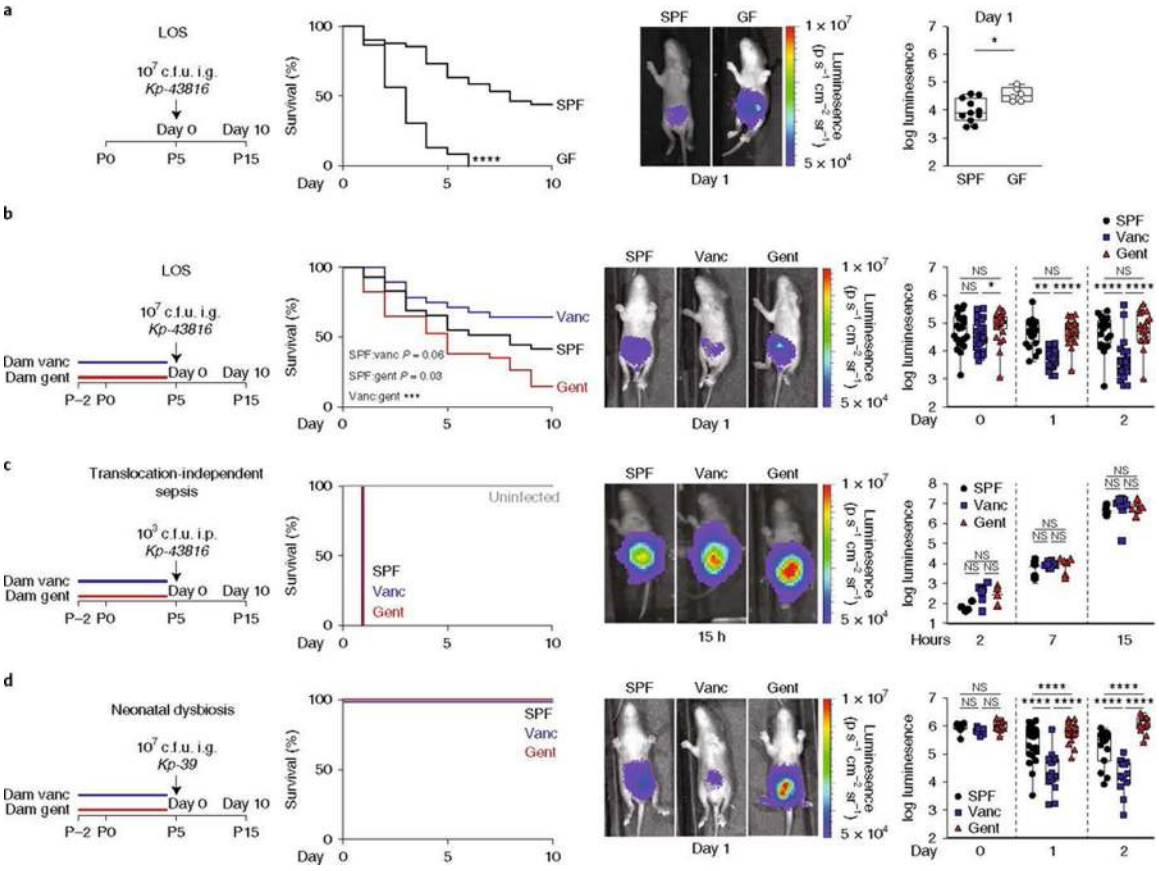

Fig. 2 |. The microbiome alters susceptibility to LOS and neonatal dysbiosis.

a, Litters of pups from SPF or GF dams were infected i.g. with 10^7 c.f.u. *Kp-43816*^{lux} on P5 and monitored daily for sepsis (Kaplan–Meier curve). Representative abdominal bioluminescence before the development of sepsis is shown and quantified. For survival analysis, data were pooled from three independent experiments with SPF ($n = 41$) and GF ($n = 23$) pups. For abdominal bioluminescence, data were pooled from four litters in three independent experiments with SPF ($n = 15$ pups of either sex) and GF ($n = 11$ pups of either sex). **b**, Littermate dams were separated 1–2 d before delivery, and drinking water was supplemented with vancomycin (vanc) or gentamicin (gent) or was left unchanged until P4. On P5, pups were infected i.g. with 10^7 c.f.u. *Kp-43816*^{lux} and monitored daily for sepsis (Kaplan–Meier curve). Representative abdominal bioluminescence before the development of sepsis is shown and quantified. For survival analysis, data were pooled from five independent experiments with SPF ($n = 29$), vancomycin ($n = 28$) and gentamicin ($n = 34$). For abdominal bioluminescence, data were pooled from four independent experiments with SPF ($n = 22$), vancomycin ($n = 28$) and gentamicin ($n = 25$). NS, not significant. **c**, Pups from antibiotic-treated littermate dams (as in **b**) were infected i.p. on P5 with 10^3 c.f.u. *Kp-43816*^{lux} and monitored for sepsis (Kaplan–Meier curve). Representative bioluminescence is shown and quantified. Data are representative of two independent experiments with SPF ($n = 6$), vancomycin ($n = 8$) and gentamicin ($n = 7$). **d**, Pups from antibiotic-treated littermate dams (as above) were infected i.g. on P5 with 10^7 c.f.u. *Kp-39*^{lux} and monitored for sepsis (Kaplan–Meier curve). Representative abdominal bioluminescence

is shown. Box-and-whisker plots show median and IQR, with lines extending to the first and fourth quartiles. Data were pooled from three independent experiments with SPF ($n = 22$), vancomycin ($n = 18$) and gentamicin ($n = 21$). In all instances, n refers to the number of pups of either sex. *$P \leq 0.05$; **$P \leq 0.005$; ***$P \leq 0.0005$; ****$P \leq 0.0001$.

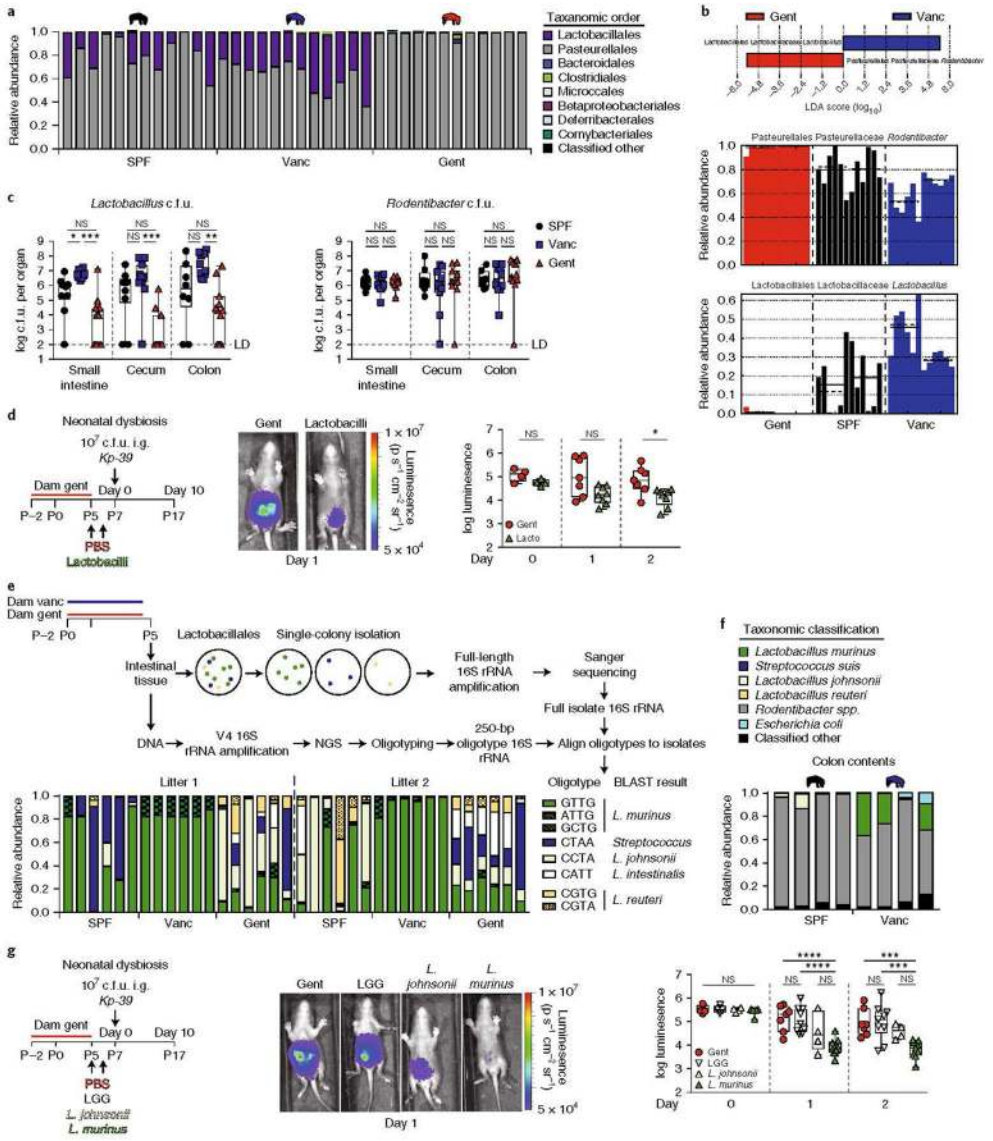

Fig. 3 |. Perinatal antibiotics alter communities of endogenous lactobacilli.

a, Relative abundances of order-level taxonomies from a 16S rRNA gene survey of intestinal microbiome communities of P5 pups reared with or without maternal antibiotic treatments: SPF (black), vancomycin (blue) and gentamicin (red). **b**, Linear discriminant analysis (top) and relative abundances of differentially abundant features (bottom) of 16S rRNA microbiome survey data. For 16S microbiome analysis, data were pooled from two independent experiments. Samples were processed and sequenced independently (2 years apart); FASTQ files were combined before analysis with $n = 12$ samples per group. Linear discriminant analysis effect size (LEfSe) analysis was performed on taxonomic classifications after the Nephele DADA2 pipeline. LDA, linear discriminant analysis. **c**, Whole intestinal organs from uninfected P5 pups reared with or without maternal antibiotics were homogenized in PBS, diluted and plated on MRS or BHI agar for selective growth of Lactobacillales and identification of *Rodentibacter* spp., respectively. After 24 h, colonies

were counted and c.f.u. per gram of tissue was determined. Data were pooled from three independent experiments with SPF ($n = 9$), vancomycin ($n = 11$) and gentamicin ($n = 11$). LD, limit of detection. **d**, Gent pups received PBS or a mixed community of lactobacilli (lacto) selectively cultured from vanc pup colon contents. Abdominal bioluminescence was measured daily. Data were pooled from two independent experiments of within-litter controls with gentamicin ($n = 7$) and lactobacilli ($n = 8$). NS, not significant. **e**, A schematic illustration depicting the combination of oligotyping analysis of 16S rRNA microbiome data from **a** with full 16S sequencing of c.f.u. isolates from **c** to determine how antibiotic rearing altered populations of endogenous lactobacilli. NGS, next-generation sequencing. **f**, Relative abundance of bacterial taxa from metagenomic sequencing of pup colon contents. For metagenomics analysis, data were from two pups per litter in two litters of either SPF or vancomycin-reared pups. **g**, Littermate gent pups received PBS or *L. rhamnosus* (LGG), *L. johnsonii* (G2A) or *L. murinus* (V10) i.g. before infection with 10^7 c.f.u. *Kp-39*^{lux}. Abdominal bioluminescence was measured daily. Box-and-whisker plots show the median and IQR, with lines extending to the first and fourth quartiles. Data were pooled from two independent experiments of within-litter controls with gentamicin ($n = 7$), *L. rhamnosus* ($n = 9$), *L. johnsonii* ($n = 4$) and *L. murinus* ($n = 9$). In all instances, *n* refers to the number of pups of either sex. $^*P \leq 0.05$; $^{**}P \leq 0.005$; $^{***}P \leq 0.0005$; $^{****}P \leq 0.0001$.

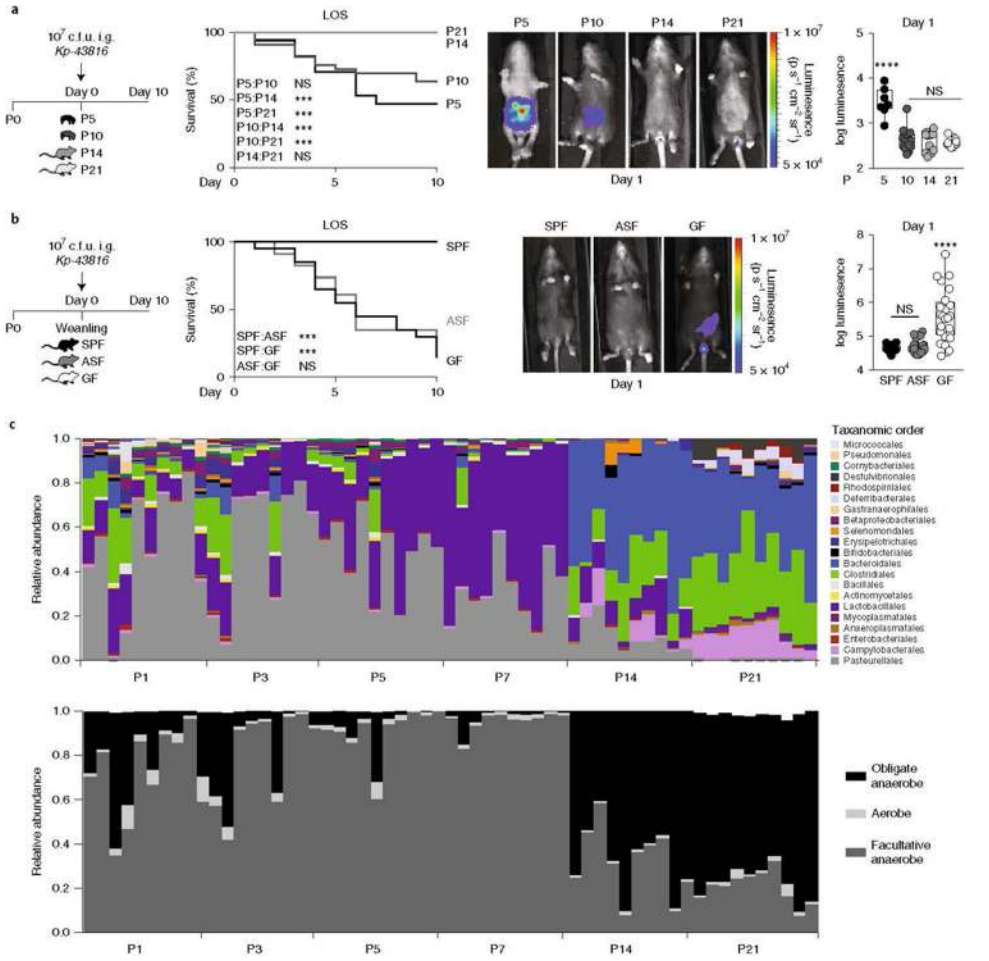

Fig. 4 |. A microbiome dominated by obligate anaerobes provides resistance to LOS.

a, Litters of pups from SPF dams were infected i.g. with 10^7 c.f.u. *Kp-43816*^{lux} on P5, P10, P14 or P21 and monitored daily for sepsis (Kaplan–Meier curve). Representative abdominal bioluminescence before the development of sepsis is shown and quantified. For survival analysis, data were pooled from two or three independent experiments per age with P5 (n = 18), P10 (n = 33), P14 (n = 15) and P21 (n = 18). For abdominal bioluminescence, data were pooled from two independent experiments with P5 (n = 7), P10 (n = 13), P14 (n = 11) and P21 (n = 10). NS, not significant. **b**, SPF or GF mice of weaning age were infected i.g. with 10^7 c.f.u. *Kp-43816*^{lux} and monitored daily for sepsis (Kaplan–Meier curve). Representative abdominal bioluminescence before the development of sepsis is shown and quantified. Data were pooled from two independent experiments with SPF (n = 12), ASF (n = 20) and GF (n = 23). **c**, Top, relative abundances of order-level taxonomies from a 16S rRNA gene survey of intestinal microbiome communities from birth until weaning. Bottom, relative abundance of genus-level taxonomies grouped by oxygen requirement. Box-and-whisker plots show the median and IQR, with lines extending to the first and fourth quartiles. Samples were collected, processed and sequenced in the same experiment spanning the course of 3 weeks with P1 (n = 6), P3 (n = 9), P5 (n = 10), P7 (n = 10), P14 (n = 10) and P21 (n = 10). In all instances, n refers to the number of pups of either sex. $^{**}P \leq 0.005$; $^{***}P \leq 0.0005$; $^{****}P \leq 0.0001$.

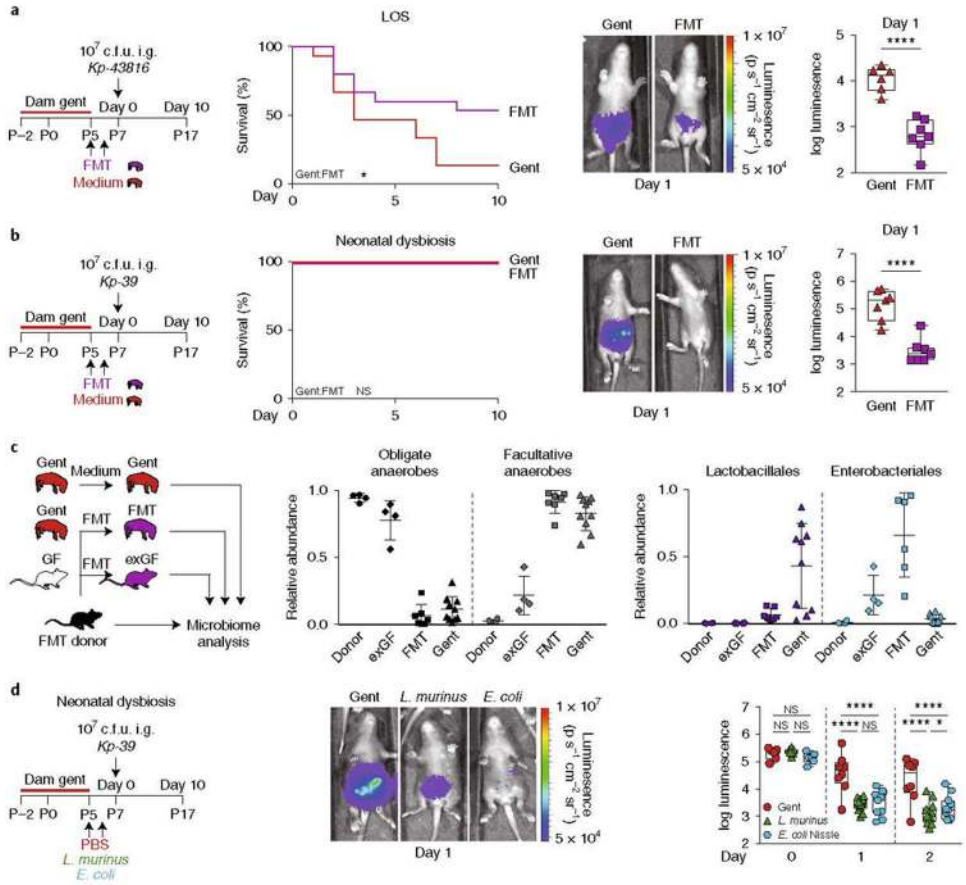

Fig. 5 |. Obligate anaerobes cannot engraft into susceptible pups to protect against LOS and neonatal dysbiosis.

a,**b**, Gent pups received medium or FMT from P19 donor feces before infection with 10^7 c.f.u. *Kp-43816*^{lux} (**a**) or *Kp-39*^{lux} (**b**; from Fig. 3g) and were monitored daily for sepsis (Kaplan–Meier curve). Representative abdominal bioluminescence before the development of sepsis is shown and quantified. For the survival analysis in **a**, data were pooled from three independent experiments with gentamicin ($n = 15$) and FMT ($n = 15$). For abdominal bioluminescence, data are representative of two independent experiments with gent ($n = 6$) and FMT ($n = 7$). Data in **b** were pooled from two independent experiments of within-litter controls with gentamicin ($n = 7$) and FMT ($n = 7$). These data were generated and analyzed with the data in Fig. 3h. NS, not significant. **c**, Left, medium or FMT from a P19 donor (donor) was delivered i.g. on P5 and P6 to gentamicin-reared pups (FMT) or to GF adults (exGF). The following day, DNA from the intestines of pups and feces from adults were subjected to a a 16S rRNA gene survey of intestinal microbiome communities. Right, relative abundance of genus-level taxonomies grouped by oxygen requirement. Also shown is the relative abundance of the orders Lactobacillales and Enterobacteriales (mean ± s.d.). Data were pooled from two independent experiments with P19 donor feces ($n = 4$), exGF ($n = 4$), FMT ($n = 7$) and gentamicin ($n = 10$). **d**, Gent pups received PBS, *L. murinus* (V10) or *E. coli* Nissle i.g before infection with 10^7 c.f.u. *Kp-39*^{lux}. Abdominal bioluminescence was measured daily. Box-and-whisker plots show median and IQR, with lines extending to the first and fourth quartiles. Data were pooled from two independent experiments of within-

litter controls with gentamicin ($n = 8$), *L. murinus* ($n = 12$) and *E. coli* Nissle ($n = 11$). In all instances, n refers to the number of pups of either sex. *$P \leq 0.05$; ****$P \leq 0.0001$.